DUST EMISSIONS FROM UNDISTURBED AND DISTURBED SOILS: EFFECTS OF OFF-ROAD MILITARY VEHICLES

by

YOUJIE XU

B.S., South China Agricultural University, 2012

A THESIS

submitted in partial fulfillment of the requirements for the degree

MASTER OF SCIENCE

Department of Biological and Agricultural Engineering
College of Engineering

KANSAS STATE UNIVERSITY
Manhattan, Kansas

2014

Approved by:

Major Professor
Dr. Ronaldo G. Maghirang

Copyright

Acknowledgements

I would like to extend my gratitude to my dear advisor, Dr. Ronaldo G. Maghirang, for such a precious opportunity to pursue my graduate study at K-State and also for the patient guidance throughout my journey to complete my degree.

I would like to thank both Dr. John Tatarko and Dr. Larry Wagner for their support and guidance. Special thanks to Matt Kucharski and all the wind erosion group at USDA-ARS for their assistance during the experimental tests. Special thanks also to Dr. Larry Hagen for his assistance in analyzing the data and to Jeremy Meeks for developing and establishing the set up and protocol for sampling.

I would like to thank Dr. James Steichen for being in my committee. I would like to thank both Dr. Leigh Murray and Nicholas Bloedow for their assistance in analyzing the data.

I would like to thank my family and friends here and also in China for their love and encouragement. Finally, I would like to acknowledge the U.S. Department of Defense Strategic Environmental Research and Development Program (SERDP), USDA ARS, and Kansas Agricultural Experiment Station - for providing the funding for this project.

Abstract

Military training lands can be significant sources of fugitive dust emissions due to wind erosion. This study was conducted to determine dust emission potential of soils due to wind erosion as affected by off-road military vehicle disturbance. Multi-pass traffic experiments using two types of vehicles (i.e., wheeled and tracked) were conducted on six soil textures at four military training facilities: Fort Riley, KS; Fort Benning, GA; Yakima Training Center, WA; and White Sands Missile Range (WSMR), NM. Prior to and after the preselected number of vehicle passes, soil samples at three locations were collected with minimum disturbance into trays. Adjacent to the location where tray samples were collected, a Portable In-Situ Wind Erosion Lab (PI-SWERL) was used to measure dust emission potential. The tray samples were tested in a laboratory wind tunnel (with sand abrader) for dust emission potential using a GRIMM aerosol spectrometer and gravimetric method with filters.

Comparison of the PI-SWERL (with DustTrak™ dust monitor) and wind tunnel (with GRIMM aerosol spectrometer) measurement results showed significant difference in measured values but high correlation, particularly for soils with high sand content. Wind tunnel tests results showed that sampling locations significantly affected dust emissions for the tracked vehicles but not for the light-wheeled and heavy-wheeled vehicles. Also, soil texture, number of vehicle passes, and vehicle type significantly affected dust emissions. For the light-wheeled vehicles, dust emissions increased as the number of vehicle passes increased. From undisturbed conditions to 10 vehicle passes, there was a significant ($P<0.05$) increase in dust emissions (297%) on average for all light-wheeled vehicle tests. From 10 to 25 passes and 25 to 50 passes, an additional 52% and 62% increments were observed. For the tracked vehicle, for the straight section sampling location, dust emission increased as the number of vehicle passes increased. However, for the curve section, dust emissions at any level of pass were significantly higher than initial condition; beyond the first pass, no significant increase was observed.

Table of Contents

List of Figures

List of Tables

Chapter 1 - Introduction

Off-road training activities at U.S. Department of Defense (US DoD) facilities are faced with environmental challenges, including ecosystem disturbance, land degradation, and environmental damages (Goran et al., 1983; Braunack, 1986; Ayers, 1994). Soil disturbance resulting from off-road military training activities can retard vegetation development, disturb wildlife habitats, and increase wind erodibility of soil. Wind erosion removes the most fertile top layer of the soil resulting in decreased soil productivity (Lyles, 1975) and air quality impairment due to fugitive dust emissions. To maintain sustainable training lands, military installations should comply with environmental regulations including the National Ambient Air Quality Standards (NAAQS) (US-EPA, 2011). Air quality issues created by off-road military training activities has been a concern for years; however, fugitive dust emissions data are needed to quantify and assess the impact generated by these activities. Additionally, better prediction models of disturbed lands are needed to aid military training land managers in planning the training timetable of military lands and also reserving the more frequently trained areas to recover into their sustainable conditions.

Several studies have been conducted to assess the impact of military training activities on training lands. Research has generally been observational in nature and the specific training activities or typical vehicle type directly creating the impacts were generally unknown in terms of their magnitude, extension and dust event frequency (Goran et al., 1983; Diersing and Severinghaus, 1984; Braunack, 1986). As such, research to establish the environmental impacts of military training activities is needed.

Recently, studies have been carried out to quantify impacts and extend the knowledge base by including more military installations over a wide range of climatic zones, soil textures, and vehicle types (Goran et al., 1983; Braunack, 1986; Horn et al., 1989; Nickling and Gillies, 1989; Grantham et al., 2001; Althoff et al., 2010; Meeks, 2013; Retta et al., 2013). These studies have assessed the impact of specific vehicles (tracked or wheeled vehicles) and intensity of training activities on soil and vegetation resources and evaluate the ability of the site to sustain and recover from the impact. Dependent variables in these studies usually include a range of measures of soil and vegetation impacts within or adjacent to the trafficked areas.

This research focused on the fugitive dust emissions rather than soil quality or vegetation covers that have been widely studied (Braunack, 1986; Horn et al., 1989; Grantham et al., 2001; Retta et al., 2013). Dust emission due to wind erosion is influenced by various factors, including wind speed and wind direction, soil texture, aggregation, vegetation cover, degree of soil disturbance, and roughness (Nickling and Gillies, 1989; Zobeck, 1991a; Gillette et al., 2001; Alfaro et al., 2004; Meeks, 2013; Retta et al., 2013). For military training lands, the degree of soil disturbance is likely related to the type of vehicle and the number of vehicle passes (Meeks, 2013).

Meeks (2013) determined the dust emission potential of disturbed soil surfaces, as affected by soil texture and intensity of training with military vehicles. In that study, dust emission potential was characterized in terms of aerodynamic suspension of surface loose materials. As an extension of Meeks' (2013) study, this research was conducted to quantify the impact of off-road military vehicle traffic disturbance on fugitive dust emissions by using sand abrader for saltating particle abrasion on undisturbed and disturbed soil surfaces. The effects of soil texture, traffic intensity, traffic pattern, and vehicle type on dust emission potential were considered.

Chapter 2 - Literature Review

2.1 Off-Road Military Vehicle Activities

The United States Department of Defense (U.S. DoD) conducts military training and testing activities on approximately 12.1 million hectares of land throughout the nation (US-DoD, 2013). These activities can result in soil disturbance and air quality degradation (Goran et al., 1983; Braunack, 1986; Ayers, 1994). For example, tremendous amounts of fugitive dust can be emitted by military vehicle disturbance and subsequently by wind erosion from disturbed soil surfaces (Gillies et al., 2005; Padgett et al., 2008). Dust entrained by wind erosion can impact the near-source areas and be transported further downwind (Gillette, 1981), which may present health threat to animals and humans (Padgett et al., 2008; Pope et al., 1995). Frequently trafficked maneuver areas are more vulnerable to wind erosion than less trafficked areas (Grantham et al., 2001; Belnap et al., 2007; Althoff et al., 2010).

Vehicle traffic, especially by heavy tracked vehicles, can cause soil surface crust disruption, large aggregate breakdown, vegetation cover removal, and soil surface smoothing (Goran et al., 1983; Diersing and Severinghaus, 1984; Braunack, 1986; Zobeck and Fryrear, 1986). Soil displacement and soil compaction resulting from vehicle traffic have a negative effect on soil quality, decreasing the biological production for vegetation growth (Goran et al., 1983; Retta et al., 2013).

The damages resulting from vehicular traffic is determined by the static and dynamic properties of vehicles including the contact area, surface pressure, total weight, track design, vehicle speed, turning radius and driving pattern (Horn et al., 1989). The surface pressure produced by vehicles at a lower driving speed is relatively higher than at a higher speed. As the surface pressure increases, the bulk density will increase (Horn et al., 1989). Tracked vehicles, which are generally heavier than most wheeled vehicles and have large track treads, have been found to produce more shear force on the soil surface when making turns than straight driving, which removes most vegetation on the soil surface (Grantham et al., 2001; Retta et al., 2013). Goran et al. (1983) observed the impacts from tracked vehicle activity at 12 training installations. Single vehicle straight-line traffic generally resulted in minor soil disturbance and light damage to vegetation, while making turns caused severe damage to vegetation and significant soil disturbance. Ayers (1994) found that sharper turns increased soil disturbance and track rutting.

Radforth (1973) also found that the amount of vegetation loss resulting from vehicle traffic depended on the surface load, with heavier vehicles causing more damage than lighter vehicles.

2.2 Ecosystem and Environmental Damages of Off-road Military Vehicles

Military vehicle traffic can drastically change the soil structure, vegetation cover and even wildlife habitat, thus adversely affecting the overall natural environmental condition for animals and humans. Goran et al. (1983) found that vegetation growth and soil quality on frequently used training areas tended to degrade when compared to non-training or less frequently training areas. Military vehicles, especially tracked vehicles, tend to damage the brush canopy and native grasses and also cause vegetative root exposure (Ayers, 1994). Generally, biomass like flora on the frequently trained areas will be reduced because the young seedlings are not able to survive under the vehicle's repeated driving. Vegetation cover plays an important role in protecting the soil surface from wind erosion by reducing the shear at the surface caused by the wind force, providing a shelter for particles on the soil surface and also trapping saltating particles. Once vegetation cover is removed by vehicle traffic, the soil surface will become more susceptible to wind erosion. Grantham et al. (2001) showed that the vertical vegetation cover was reduced as tracked vehicle passes increased and threshold wind speed significantly decreased, resulting in increased total soil loss.

Diersing et al. (1984) found that on short-grass prairie, vegetation cover decreased on the trained areas. Breakdown of soil aggregates and increases in bulk density were also observed on the training areas. Bulk density of disturbed areas by tracked vehicles was found to increase compared to the adjacent undisturbed areas (Braunack, 1986; Retta et al., 2013). Retta et al. (2013) reported that the M1A1 tank traffic passes had a significant effect on the soil bulk density and vegetation covers at Fort Riley, KS. Continued vehicle impact could limit the vegetation and root growth due to soil compaction, further accelerating soil degradation and reducing the usefulness of a site for training activities.

2.3 Dust Emissions from Military Training Lands

Off-road vehicle activities are a source of considerable fugitive dust emissions that are under regulatory control (i.e., PM_{10} (particulate matter with equivalent aerodynamic diameter of 10μm or less) and $PM_{2.5}$ (particulate matter with equivalent aerodynamic diameter of 2.5μm or less)) (US-EPA, 2011). Primary emissions of loose particles from the soil surface can be generated by mechanical suspension or wind erosion. Wind erosion can suspend particulates into the air to a high enough concentration level to cause visibility hazards (Hagen and Skidmore, 1977). Padgett et al. (2008) monitored fugitive dust emissions from vehicles traveling on dry, unpaved roads and found that smaller particles can travel at least 100 m away from the source and also the dust concentrations may threaten drivers' health. Yamaguchi et al. (2012) demonstrated that Asian dust originated from the arid regions and deserts of China and Mongolia can be transported long-distance to Japan, especially small dust particles (< 1μm). The breakdown of aggregates into smaller particles and the resulting dust may induce inflammatory diseases in nasal mucous membranes and get deep into the lungs. Fine particles ($PM_{2.5}$) can get deep into the lung system and lead to cardiopulmonary mortality (Pope et al., 1995; Schwartz et al., 1996). High PM concentration in ambient air is believed to cause cardiovascular disease and premature death (Green and Armstrong, 2003; Timonen et al., 2006).

Military training and testing ranges have the potential for considerable dust emissions generated by mechanical disturbance and subsequently by wind erosion from disturbed soil surfaces (Gillies et al., 2005; Padgett et al., 2008). Large amounts of particulate matter can be generated during military training exercises where wheeled and tracked vehicles are used.

Fine particle emission by wind erosion is highly dependent on soil texture, wind speed and mineralogy (Gillette, 1977). The condition of the soil and vegetation before and after vehicle traffic plays a big role on the amount and length of time that dust could be potentially emitted from these disturbed areas. Many activities take place on military training sites including industrial, commercial and residential activities including heavy munitions and vehicle training activities. Many military installations are located in, or near, existing or proposed air quality non-attainment areas, which may not comply with the NAAQS (Table 2-1). Military training activities could be a large source for fugitive dust emissions that are under regulatory control (i.e., PM_{10} and $PM_{2.5}$) and have the potential to impact the local and regional air quality.

Table 2-1. National ambient air quality standards for particulate matter (PM_{10} and $PM_{2.5}$) (US-EPA, 2011).

Pollutant*	Primary/ Secondary	Averaging Time	Level	Form
$PM_{2.5}$	primary**	Annual	12 μg m^{-3}	annual mean, averaged over 3 years
	secondary***	Annual	15 μg m^{-3}	annual mean, averaged over 3 years
	primary and secondary	24-hour	35 μg m^{-3}	98th percentile, averaged over 3 years
PM_{10}	primary and	24-hour	150 μg m^{-3}	not to be exceeded more than once per year on average over 3 years

* As of Dec. 14, 2012

**Primary standards provide public health protection, including protecting the health of "sensitive" populations such as asthmatics, children, and the elderly.

***Secondary standards provide public welfare protection, including protection against decreased visibility and damage to animals, crops, vegetation, and buildings.

2.4 Wind Erodibility of Soil

Soil erosion by wind is a serious problem in many flat, bare, arid lands throughout the world. Wind erosion first removes the surface soil containing many nutrients necessary for vegetation growth and leads to poor productivity for future plants (Lyles, 1975; Zobeck and Fryrear, 1986; Hagen et al., 1996; Belnap and Gillette, 1998). Suspended dust can cause severe air pollution and damage plant leaves by particle abrasion (Armbrust, 1982; Sharratt and Lauer, 2006). Once the wind strength exerted on the soil particle is sufficient to lift the particle, it will begin to move. Large particles will roll or hop on the soil surface if no vegetation cover protection is present, then smaller particles will be suspended and transported further downwind.

A minimum wind speed is required to initiate soil particle movement according to soil textures and soil surface condition such as surface roughness (Gillette et al., 1982).

Wind erosion processes and consequent dust emissions are fairly well established (Hagen, 1991; Mirzamostafa et al., 1998; Hagen, 1999). Bagnold (1941) identified three particle transport modes contributing to wind erosion: suspension, saltation, and creep (Figure 2-2). Most soil movement by wind is entrained and transported by particle saltation, a bouncing motion of windblown grains (Bagnold, 1941; Shao et al., 1993; Eames and Dalziel, 2000). Saltating soil particles are lifted up into the air and then drop back to the surface as they are too heavy to remain suspended, which can cause additional saltating particles. These particles may impact and cause smaller particles to become suspended into the atmosphere (Gillette, 1981; Shao et al., 1993; Rice et al., 1996). Saltation impact is well recognized as the principal mechanism by which dust sized particles are ejected into air in many arid environments (Gillette, 1977; Shao et al., 1993).

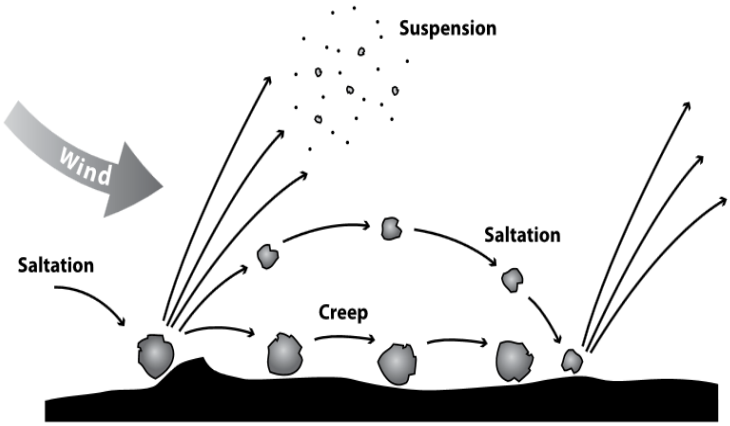

Figure 2-1. Particle transport modes under wind erosion (taken from Presley and Tatarko, 2009).

According to Mirzamostafa et al. (1998), three major sources of suspension-size dust (SSD) generated during wind erosion include direct emission of loose SSD, abrasion of SSD from surface clods and crust by saltating bombardment, and breakdown of particles and saltating aggregates. Dust can be lifted up by aerodynamic suspension of loose erodible material or by dynamic entrainment associated with saltating particles. Aerodynamic entrainment is governed

by wind shear stress and characterized as the threshold shear velocity (Gillette et al., 1982; Nickling and Gillies, 1989; Belnap and Gillette, 1997). Aerodynamic entrainment of dust involves the direct emission of loose suspension-size dust in the absence of abrasion and splashing dust impacted by saltating grains (Mirzamostafa et al., 1998). Sediment is lifted from soil surfaces when the wind speed exceeds the threshold friction velocity at the soil surface (the minimum wind velocity required to detach particles from the soil surface and emit them into the atmosphere).

Previous studies on aerodynamic entrainment of dust have demonstrated that an initial dust emission with rapid decay to zero within 2 or 3 minutes can be observed (Chepil and Woodruff, 1963; Shao et al., 1993; Loosmore and Hunt, 2000; Houser and Nickling, 2001a; Macpherson et al., 2008; Baddock et al., 2011). In one study from supply-limited surfaces, dust emissions were found to be mainly driven by direct aerodynamic suspension of surface loose erodible material and not by the dynamic entrainment mechanisms through sandblasting (Macpherson et al., 2008). Dynamic entrainment occurs in the presence of saltating sand grain when its kinetic energy is strong enough to break the interparticle bonding of surface sediments (Macpherson et al., 2008). Saltation-size particles move more easily than dust-size particles because cohesive forces such as Van der Walls forces and cementation are stronger among dust than saltating particles (Loosmore and Hunt, 2000).

The high-magnitude, low-frequency dust storm events are often driven by dynamic entrainment through saltation abrasion, whereas, high-frequency and low dust emission and high ambient dust concentration are mostly contributed by the aerodynamic entrainment process (Lee and Tchakerian, 1995; Houser and Nickling, 2001b; Macpherson et al., 2008; Baddock et al., 2011). In some arid areas, the aerodynamic entrainment of dust may dominate during dust storm event (Kjelgaard et al., 2004).

Many factors can influence wind erosion processes and the resulting fugitive dust emissions. Hagen (1991, 2004b) conducted a series of studies to understand the physical interaction among the soil, particles, and wind, including the abrasion of aggregated and crusted soil and fine particles generated by the mobile aggregate breakdown. A wind erosion model, the Wind Erosion Prediction System (WEPS), was developed to predict the soil loss and dust emission on cropland fields (Hagen et al., 1999; Hagen, 2004a). The WEPS model has the

potential to simulate the military training activities and predict fugitive dust emission generated by military vehicles.

Soil surface roughness, crust development, and soil moisture are major factors that influence a soil's erodibility to wind (Nickling and Gillies, 1989; Zobeck, 1991a; Alfaro et al., 2004). Soil crusting is important to inhibit fine and coarse particle emissions as it consolidates the soil surface material compared to loose surface soils (Gillette et al., 1982; Zobeck, 1991b; Goossens, 2004). Gillette et al. (1982) tested the effect of soil crusting, particle abrasion, wind speed and soil textures on fine particle production and found that fine particle fluxes were highly dependent on wind speed but relatively independent of sand abrasion and soil texture. Shao et al. (1993) reported that at least a 7 m wind tunnel length was required to study the saltation effect in an equilibrium state and that the emission of dust particles by saltation impact (as opposed to loose dust particles lifted by aerodynamic forces) is the principal mechanism for the natural entrainment of dust by wind.

Vegetation cover on the soil surface can reduce soil erosion by wind in several ways: (1) vegetation protects the soil surface and shelters soil particles from wind; (2) vegetative leaves absorb wind momentum and subsequently reduce surface wind shear stress; (3) vegetative root with water can consolidate the soil structure and make the soil more cohesive; and (4) vegetation can trap the airborne particles (Chepil et al., 1963; Woodruff and Siddoway, 1965).

Soil moisture is significant for crust development and aggregate formation through the cohesive forces among the particles. As soil surface moisture changes according to atmospheric humidity, Ravi et al. (2004) showed that air humidity has a significant effect on the soil susceptibility to wind erosion.

Soil surface disturbance, e.g., by vehicles, is another important factor that influence wind erosion. Disturbance can alter the soil surface characteristics such as vegetation and soil structure, which may cause accelerated soil loss by wind erosion (Belnap, 1995). Disturbance by livestock or vehicle traffic over soil crusts was found to supply more sediment and leave the soil surface to be more vulnerable to wind erosion in sandy loam soils (Belnap and Gillette, 1997; Macpherson et al., 2008). Belnap and Gillette (1998) found that threshold friction velocity of disturbed soils is much lower than that of undisturbed biological soil crusts. Macpherson et al. (2008) also found that disturbance of the soil surface would increase the potential for multiple dust emission events.

Chapter 3 - Materials and Methods

3.1 Field Sites

Field experiments were conducted on four U.S. DoD military training sites, including Ft. Riley (FR), KS, Ft. Benning (FB), GA, Yakima Training Center (YTC), WA, and White Sands Missile Range (WSMR), NM (Figure 3-1). Two soil textures were identified for testing at FR and WSMR, with one soil texture from each of the other two sites (Table 3-1; Figure 3-2). Briefly, military vehicles (Figure 3-3) were driven on each site for a specific set of vehicle passes. After each pass, soil samples were carefully removed and placed into the wind tunnel trays for dust emission testing in a laboratory wind tunnel located at the USDA-ARS Center for Grain and Animal Health Research (CGAHR), Manhattan, KS. Laboratory wind tunnel tray experiments were conducted to evaluate the fugitive dust emission potential under a non-abrader conditions and then also by supplying saltation (i.e., abrader tests).

.

Figure 3-1. Experimental sites of the four military training installations: (A) Ft. Riley, KS; (B) Ft. Benning, GA; (C) Yakima Training Center, WA; and (D) White Sands Missile Range, NM.

Table 3-1. Particle size analysis of soil samples from four experimental sites.

Experimental Site	Soil Texture	Clay* (%)	Silt* (%)	Sand* (%)
Ft. Riley, KS	silt loam	19.0±4.8	70.7±4.1	10.2±1.1
	silty clay loam	28.0±5.7	64.1±5.6	7.9±1.3
Ft. Benning, GA (Rowan Hill)	loamy sand	2.8±1.0	9.5±1.7	87.7±2.4
Yakima Training Center, WA	sandy loam	5.0±1.0	43.8±3.4	51.3±3.2
White Sands Missile Range, NM	loam	21.9±3.5	39.7±10.0	38.4±9.6
	sandy loam	7.7±1.3	19.3±3.7	73.0±4.8

*Particle size determined by pipette method of (Gee and Dani 2002).

±Denotes standard deviation values of six replicate.

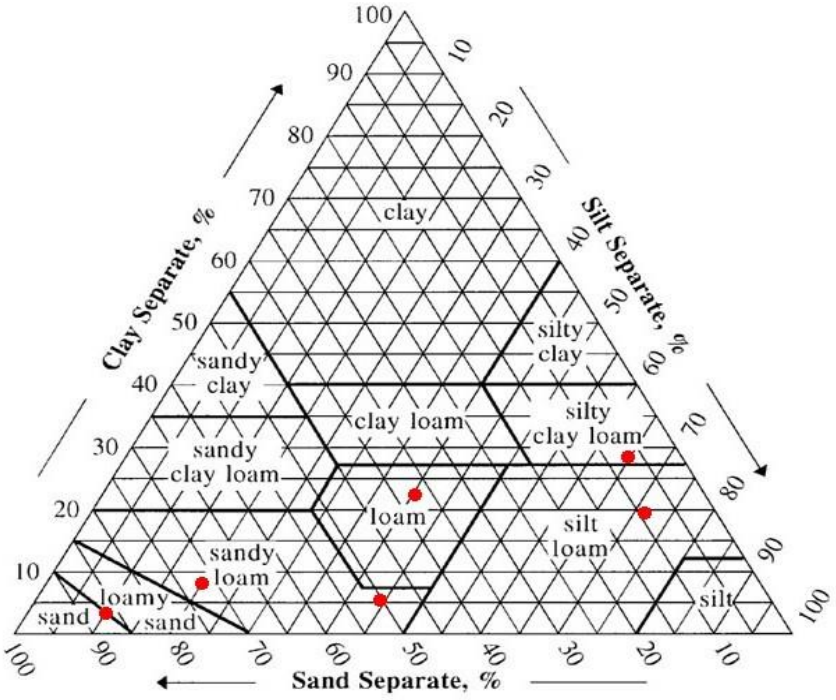

Figure 3-2. Soil textures at the experimental sites.

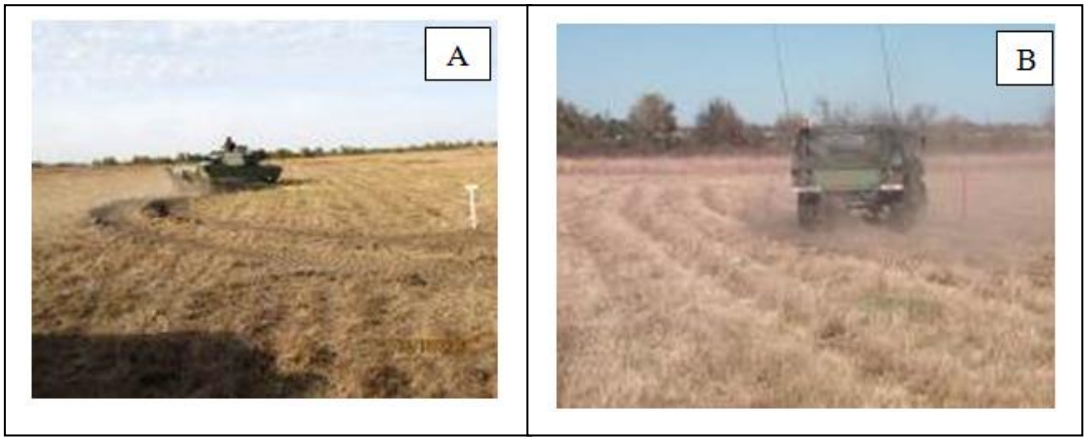

Figure 3-3. Military vehicles used at Ft. Riley, KS: (A) tracked; and (B) light-wheeled.

Two types of off-road military training vehicles (i.e., tracked and wheeled) were selected for each site, except at YTC in which two types of wheeled vehicles (i.e., heavy and light) were used. At the YTC site, a heavy-wheeled vehicle (i.e., fire truck) was used instead because a tracked vehicle was not available at the time of testing. These represented a range of relatively lightweight to very heavy, fully armored military off-road vehicles (Table 3-2).

Table 3-2. Vehicle types and testing dates for this study.

Vehicle	Traction Type	Mass (kg)	Fort Riley (FR)	Fort Benning (FB)	Yakima Training Center (YTC)	White Sands Missile Range (WSMR)
M1025A2 HMMWV*	Wheeled	3,075	Nov. 2010		Aug. 2012	
M1A1 Abrams Tank	Tracked	61,325	Oct. 2010	Jul. 2012		
M88A1 Tank Retriever	Tracked	50,800				Jan. 2014
M1151A Up-armored HMMWV	Wheeled	3,697		Jul. 2012		Jan. 2014
M925A1 Fire Truck	Wheeled	15,100			Aug. 2012	

*HMMWV refers to High Mobility Multipurpose Wheeled Vehicle.

3.1.1 Wind Tunnel Tray Sampling

A completely randomized experimental design consisting of three levels of vehicle passes as well as the initial condition was conducted in each soil texture at the four military training installations. Within each rectangular plot (40m×80m), a figure-8 traffic pattern with inside turning radius of 10 m was driven by vehicles (either tracked or wheeled vehicle) repeatedly to provide multiple-pass level data in both turning and straight line traffic configurations (Figure 3-4).

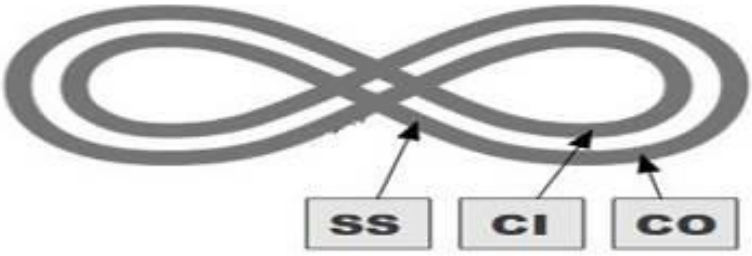

Figure 3-4. Figure-8 plot showing tray sample extraction locations. SS is straight section, CI is curve inside, and CO is curve outside.

The number of trafficking passes for each vehicle was initially determined from preliminary tests at FR to represent minimum measurable, moderate, and severe impact upon the soil and surface state. The M1A1 Abrams Tank (tracked vehicle) is much heavier than the HMMWV vehicle (light-wheeled vehicle), imposing greater lateral shear, which subsequently creates more disturbance to the soil surface in the curved sections of the figure-8. Thus, the M1A1 tank on the "tracked" plots were trafficked 1, 4, and 5 times during the three sets of passes for a cumulative total of 1, 5, and 10 passes at the conclusion of each set of passes. Because the HMMWV vehicles caused significantly less disturbance to the soil surface, the HMMWV on the "wheeled" plots was trafficked 10, 15, and 25 times during the three passes for a cumulative total of 10, 25, and 50 trafficking passes at the conclusion of each set of passes. Likewise, the M925A1 fire truck (heavy-wheeled vehicle) at YTC was trafficked 2, 8 and 10 times during the three passes for a cumulative total of 2, 10, and 20 trafficking passes at the conclusion of each set of passes. The M88A1 Tank Retriever (tracked vehicle) at WSMR was trafficked the same as the M1A1 Abrams Tank since they were similar sized vehicles. Table 3-3 lists the vehicle passes summary at each site/vehicle combination.

Table 3-3. Traffic intensity levels (vehicle passes) at each site and vehicle combination.

Location (Vehicle)	Initial Condition (passes)	Low Traffic Intensity (passes)	Medium Traffic Intensity (passes)	High Traffic Intensity (passes)
Ft. Riley (HMMWV)	0	10	25	50
Ft. Riley (M1A1)	0	1	5	10
Ft. Benning (up-armored HMMWV)	0	10	25	50
Ft. Benning (M1A1)	0	1	5	10
Yakima Training Center (HMMWV)	0	10	25	50
Yakima Training Center (M925A1 Fire Truck)	0	2	10	20
White Sands Missile Range (HMMWV)	0	10	25	50
White Sands Missile Range (M88A1)	0	1	5	10

Before vehicle traffic, an initial set of wind tunnel tray samples was collected within each plot. These initial samples were referred to as the "control" or "undisturbed" condition to determine a baseline for the original soil status. In each of the figure-8 plots (Figure 3-4), soil samples were collected from three sampling locations (i.e., SS, CI, CO) within the vehicle tracks after each set of passes. At each sampling location, the top 6-cm soil was carefully removed from a 122 cm×20 cm area with the assist of a specially-made shovel and placed into a wooden wind tunnel tray of equal size (Figure 3-5). At each site, there were three replications for each vehicle/soil texture combination. Soil surface samples (top 5 cm) were also collected in the field, air-dried and sieved by a rotary sieve with size of 0.42, 0.84, 2.00, 6.35, 19.06, 44.45, and 76.20 mm (Lyles et al., 1970). Aggregate <0.84 mm fraction was determined to represent the wind erodible fraction. Random roughness (RR) is defined as the standard error of individual elevations after oriented roughness has been removed (Zobeck and Onstad, 1987). Random roughness was measured using a pinmeter with 101 pins separated 1 cm from each other (Wagner and Yu, 1991).

Figure 3-5. Wind tunnel tray sample extracted from Yakima Training Center, WA.

Each tray was wrapped with aluminum foil and plastic wrap to reduce the disturbance during the transportation back to the laboratory (Figure 3-6). The trays were then stored in a greenhouse (Figure 3-7) to allow air drying at least one month before any testing in the wind tunnel.

Figure 3-6. Wind tunnel tray storage rack.

Figure 3-7. Wind tunnel trays in the greenhouse.

3.1.2 PI-SWERL Measurements

The dust emission potential was measured in the field using the Portable In-Situ Wind Erosion Laboratory (PI-SWERL). Dust suspension within the PI-SWERL chamber is initiated by a rotating, flat annular ring resulting in shear stress being generated at the soil surface (Schlichting and Gersten, 2000). The device has advantages of easy access to sites, low operating cost, and a greater number of tests can be done in a given time compared with a large portable or laboratory wind tunnel. However, it has the limitations of not realistically simulating a natural atmospheric boundary layer, which is related to the wind erosion process. Rather, it works on the principle of shear stress being generated at the soil surface. It has demonstrated its capability in measuring the dust emission from off-road vehicle trails on 16 arid soil types (Goossens and Buck, 2009) and characterizing the effectiveness of fugitive dust suppressants for a range of soil types (Kavouras et al., 2009). It has been applied to various desert landforms including desert pavement, loessial soils with silt-rich surficial crusts, fluvial loess with biological crusts, playas with salt or silt crust, beaches and sand dunes (Goossens and Buck, 2009; Bacon et al., 2011; Sweeney et al., 2011). A series of collocated tests correlating the PI-SWERL to a portable straight-line filed wind tunnel was conducted by Sweeney et al. (2008) on 32 distinct soil conditions in the Mojave Desert. The correspondence between these two measurements were high for most soil surfaces except on the densely packed gravel surfaces.

A typical PI-SWERL measurement begins with the operation of the clean air blower, flushing out any particles accumulated inside the sampling pipe. After that, a computer directs the motor to spin the annular ring to achieve a target rate of rotation specified in revolutions per minute (RPM). The target RPM may be held for certain period and then increased to another RPM level and maintained for some additional period (Step-wise Mode). A DustTrak™ monitor (TSI Inc., St. Paul, MN) measures the suspended particle and determines the PM_{10} concentration. The monitor uses 90^{o} light scattering technology to determine particle concentration and a size-selective inlet (<10 μm) was used to ensure only particles smaller than 10 μm in diameter was measured.

During the field sampling, next to each sampling location of collecting wind tunnel tray sample, a PI-SWERL measurement with a stepwise sampling mode was taken (Figure 3-8). In this mode, the sampling tube was first purged for 60 s. Then, the annular ring was initiated to accelerate for 45 s until it reached the target speed of 2000 RPM and continue running at this rate

for another 60 s. The second and third target velocities, which were also ran for 60 s each, were 3000 and 4000 RPM, respectively. The final step was to shut down the annular ring and purge the sampling tube for 60 s. A stepwise sampling mode with lower RPM levels was used on highly erodible soils at YTC and WSMR to prevent overloading the DustTrak(TM) monitor that was previously experienced at FB.

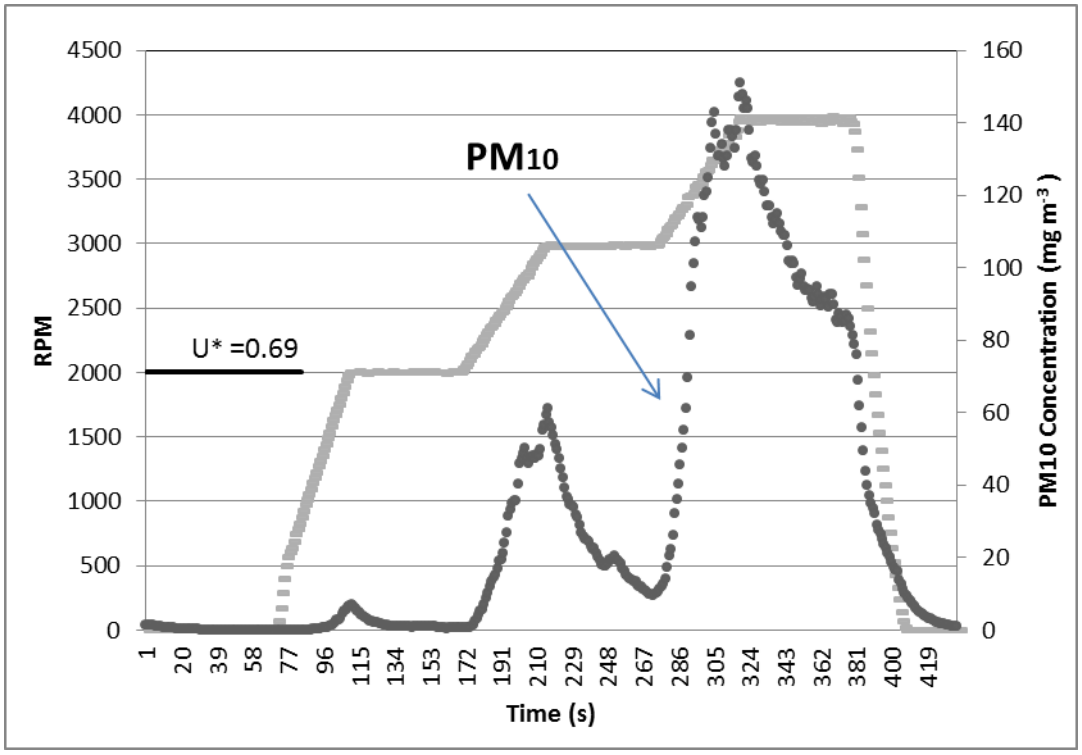

Figure 3-8. PI-SWERL stepwise test mode.

The dotted line represents the concentration of PM_{10} and the dashed line represents RPM levels. U* is estimated friction velocity (m s^{-1}).

3.2 Laboratory Wind Tunnel Measurement

3.2.1 Laboratory wind tunnel

Laboratory wind tunnels have been used to study the physics of aeolian transportation and soil entrainment among different soil textures (Bagnold, 1941; Hagen et al., 1999; Hagen 2004a; Kohake et al., 2010). They provide the following advantages: (a) the wind speed can be varied and controlled; (b) wind direction is fixed; and (c) the wind tunnel floor surface can be modified to simulate the natural surface roughness and turbulent intensity ensuring a logarithmic boundary layer has been properly developed.

The wind tunnel in this study is a variable-speed, push-type tunnel with dimensions of 12.2 m length, 1.2 m width, and 1.5 m height. Outdoor air was sucked into the wind tunnel by a variable-speed axial fan. At the upwind portion of the wind tunnel were screens to achieve a more uniform wind tunnel velocity and honeycomb structure to reduce lateral turbulence. After the honeycomb structure were spires extending from the floor surface, which were used to generate turbulence near the floor surface and slightly increase the initial boundary layer depth. Pea-sized gravel, ranging in size from 5 to 7 mm, were applied to the entire length of the tunnel floor approximately 7 m downwind of the spires to simulate roughness conditions of natural soil surfaces (1.6 mm random roughness as defined by Allmaras et al., 1966). The roughness provided boundary layer depth (approximately 0.3 m) within the air stream that better replicates those found in actual field conditions (Hagen, 1999; Kohake et al., 2010).

The wind tunnel was equipped with instrumentation for measuring temperature, humidity, atmospheric pressure, and wind speed. It is also equipped with a dust sampling system, consisting of a slot sampler and aerosol spectrometer. The instruments and dust sampling system are described below. Sampling dust in a moving air stream must be conducted under isokinetic conditions. Stetler (1997) stated that an isokinetic sampler should not interfere with or modify the passing air stream or particle motion. Anisokinetic sampling may result in a distortion of the size distribution and a biased estimate of the concentration. For example, if the air stream velocity is less than the velocity inside the sampler, measured values can underestimate true concentration because some particles with high inertia originally in the volume sampled cannot follow the converging streamlines to enter the sampler and are lost from the sample. A high-volume pump was used to develop a negative pressure in the slot sampler to match the pressure

of the moving air stream. A high-volume pump with the constant flow rate of 0.019 m^3/s was selected for this study. When conducting the wind tunnel tests for the WSMR samples, the dust sampling system setup was modified and a portion of the slot opening was blocked (0.36 m was open from the bottom) to achieve isokinetic condition.

3.2.2 Instrumentation

A differential pressure transducer (Model 264, Setra Systems) (Figure 3-9) connected to the pitot-static tube inside and outside of the slot sampler was used to measure the pressure and the free stream wind speed in the wind tunnel. The pressure transducer converts differential pressure between the two ports into a linear DC voltage signal (0 to 5 V). They are temperature compensated to 0.033% full scale/°F thermal error over the temperature range of 0°F to +150°F. The accuracy at constant temperature is ±1.0% full scale. Additionally, the pressure within and outside the slot sampler was maintained at isokinetic conditions and was continuously monitored using the transducers. A Labview program was used to monitor and display the pressure difference both inside and outside the slot.

Figure 3-9. Setra model 264 differential pressure transducer.

A temperature/humidity sensor (HUMICAP HMP 110, Vaisala) (Figure 3-10) was used to monitor the humidity and temperature during the wind tunnel testing. This sensor has a thin-film capacitive sensor with measurement ranges of 0 to 100% RH and -40 to 80°C. The humidity and temperature were measured in real-time to calculate the air density during testing.

Figure 3-10. Vaisala HMP 110 temperature and humidity sensor.

A barometer (Model PTB-110, Vaisala) (Figure 3-11) was used to measure ambient atmospheric pressure. The barometric pressure was used in calculating air density during the testing, which was subsequently used in determining wind velocity within the tunnel.

Figure 3-11. Vaisala PTB-110 electronic barometer.

An aerosol spectrometer (GRIMM Technologies Model 1.108, GRIMM GmbH) was used to measure the particle concentration (Figure 3-12). The instrument has been used in other wind erosion studies (Funk et al., 2008; Baddock et al., 2011) and works on the principle of light scattering to provide concentration of particles in 15 size ranges from 0.3µm to 20µm. This spectrometer draws air at 1.2 L/min past a light-scattering laser diode source.

Figure 3-12. GRIMM Model 1.108.

During wind tunnel testing it was important to monitor the centerline free stream velocity in the wind tunnel. A pitot tube was used in conjunction with a pressure transducer (Model 264, Setra Systems, Inc.), which had a pressure measurement range of 0 to 250 Pa and corresponding

voltage output of 1 to 5 VDC. The transducer was supplied with factory calibration curves. The air velocity was calculated using the equation (NASA, 2010):

$$V = \sqrt{\left[\frac{2(P_2 - P_1)}{\rho}\right]} \quad (3.1)$$

where:

V = air velocity (m s^{-1})
$P_2 - P_1$ = differential pressure across pitot tube (Pa)
ρ = air density (kg m^{-3}

3.3 Wind Tunnel Tray Preparation

During the wind tunnel tray sampling, significant amount of soil was collected on the edge sides of each tray. Prior to wind tunnel testing, a brush was used to clean the soil from the edge sides of the wind tunnel trays as they were not considered part of the wind tunnel tray samples (Figure 3-13).

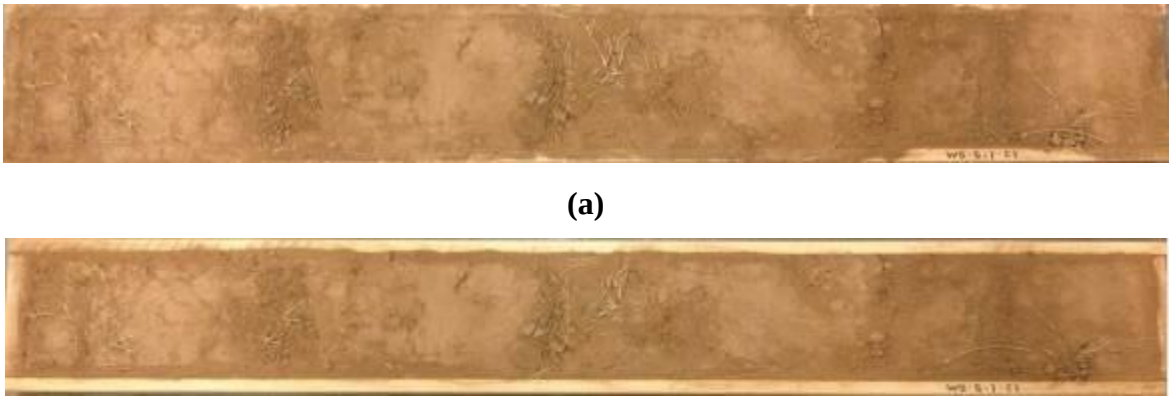

(a)

(b)

Figure 3-13. Wind tunnel tray: (a) before edge side cleaning; and (b) after edge side cleaning.

The line intercept method (Laflen et al., 1981; Sloneker and Moldenhauer, 1977) was used to estimate the vegetative cover percentage on each wind tunnel tray surface. A 100-cm ruler with 1cm interval (totally 100 points) was place on the center of the tray and each point was counted if it was in line with any vegetation residue (Figure 3-14).

Figure 3-14. Measurement of vegetative residual cover.

Each wind tunnel tray was inserted into the wind tunnel floor and a hydraulic jack under the wind tunnel tray was adjusted up and down to horizontally match the tray elevation level with the wind tunnel floor. Before the abrader test, each wind tunnel tray was subjected to a wind speed of 13 m/s for 5 min to remove and measure the loose erodible materials on the tray surface. This wind speed, as shown by Kohake et al. (2010), would remove most of the loose erodible material on the surface within 5 min of testing for the soils they tested. Besides this major source of suspension-size dust (SSD) generated during wind erosion by direct emission of loose SSD, abrasion of SSD from surface clods by saltation particle impact could cause significant amount of dust emission. Figure 3-15a represents a low erodible soil surface with high vegetation cover and Figure 3-15b represent a highly erodible soil surface with less vegetation cover. As shown in Figure 3-15a, a majority of dust was emitted from the tray surface within first 270 s, which is the dust supply-limited condition representing most of the wind tunnel tray samples. However, for those highly erodible tray samples as shown on the Figure 3-15b, after 5 min blowing there was still significant amount of dust on the tray surface. After the non-abrader test, wind tunnel trays were subjected to a fixed amount of sand abrader to further measure dust emission induced by saltation particles.

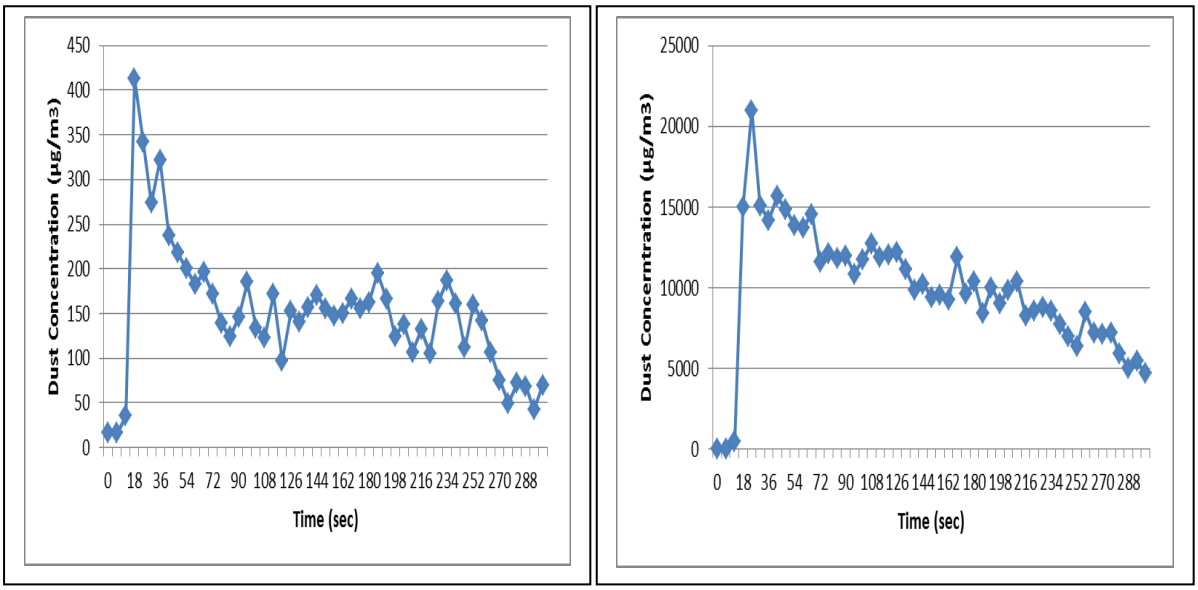

(a) (b)

Figure 3-15. Trends in measured particle concentration over 5 min for sandy loam soil at Yakima Training Center: (a) less erodible sandy loam soil; and (b) highly erodible sandy loam soil.

3.3.1 Wind Tunnel Tray Surface Condition

The vehicle traffic degraded vegetation covers on all soils for each site and also disrupted the soil surface structure as shown in Figure 3-16 to Figure 3-20. These figures show the soil surface characteristics of the initial condition as well as after each set of traffic passes were conducted at each site. In general, vegetative covers were reduced as the number of traffic passes increased. For the FR site, vegetation cover was present on the initial condition sample; after subsequent trafficking passes, the consolidation of aggregates can be seen (Figure 3-16). For the FB site, less vegetation cover was observed on the sandy soil surface than at FR (Figure 3-17); small and fragile crusted cake was found on the initial condition. For the YTC site, dense and standing vegetative cover was observed on the initial condition; plenty of vegetative cover was left on loose erodible sandy soil surface after vehicle passes (Figure 3-18). For the WSMR site, consolidated surface crust and relatively soft vegetative covers lying on the loam soil surface of the initial condition; after vehicle trafficking, crust disruption and barely vegetative covers can be seen (Figure 3-19). However, on the sandy loam soil surface, relatively less vegetative covers was found but plenty of gravels on or underneath the surface to help armor the surface (Figure 3-20).

Figure 3-16. Surface conditions of wind tunnel trays from the curve outside section trafficked by treated tracked vehicle at Fort Riley (silt loam): (A) undisturbed, (B) 1 pass, (C) 5 passes, and (D) 10 passes.

Figure 3-17. Surface conditions of wind tunnel trays from curve outside section trafficked by wheeled vehicle at Fort Benning (loamy sand): (A) undisturbed, (B) 10 passes, (C) 25 passes, and (D) 50 passes.

Figure 3-18. Surface conditions of wind tunnel trays from curve outside section trafficked by light-wheeled vehicle at Yakima Training Center (sandy loam): (A) undisturbed, (B) 10 passes, (C) 25 passes, and (D) 50 passes.

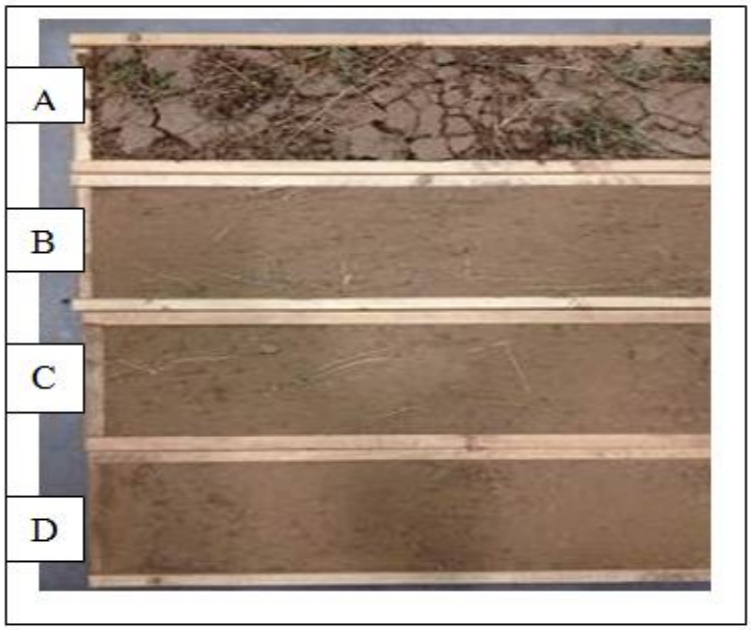

Figure 3-19. Surface conditions of wind tunnel trays from curve outside section trafficked by wheeled vehicle at White Sand Missile Range (loam): (A) undisturbed, (B) 10 passes, (C) 25 passes, and (D) 50 passes.

Figure 3-20. Surface conditions of wind tunnel trays from curve outside section trafficked by wheeled vehicle at White Sands Missile Range (sandy loam): (A) undisturbed, (B) 10 passes, (C) 25 passes, and (D) 50 passes.

3.4 Abrader Testing

Each wind tunnel tray was weighed before the abrader test to determine the initial tray weight and also after the testing to determine the final tray weight. The difference between the initial and final tray weight was considered the Total Tray Loss, which accounts for the total soil loss during the test. After air-drying wind tunnel tray samples from FR, large cracks were on the soil surface which might trap saltating particle. A soil slurry was used to fill in the cracks to create a more uniform and natural surface that would minimize the issue of trapping saltation particles.

For the wind tunnel tray samples from FR, FB, and YTC, the setup of dust sampling system was slightly different (for details refer to Meeks, 2013). For the wind tunnel trays from WSMR testing, a new setup was used as shown in Figure 3-21. The reason for updating the dust sampling system was that the diameter of the sampling duct was too large to meet the isokinetic requirement for the GRIMM spectrometer sub-sampling. Therefore, a vertical integrated slot

sampler (Figure 3-23) with a 1-m height and 5-mm wide opening slot collected sediment in suspension as well as material moving by saltation and creep at the center of the tunnel exit. The opening of the slot sampler was blocked above a height above the tunnel floor (0.36 m) and also aspirated by one high-volume pump to achieve a best possible isokineticity. Four static pressure tubes located at equal heights both inside and outside of the slot sampler (two tubes inside and two outside the slot sampler) were used to monitor wind flow and for verification wind flow was isokinetic at the sampler inlet. Total suspended PM was collected on 20 x 25 cm glass fiber filters located above the sampling pumps (Figure 3-21). The filters were humidity conditioned in a chamber calibrated to 40% relative humidity maintained with a sulfuric acid solution. Filters were conditioned for a minimum of 24 hours before taking initial weights as well as for another 24-hour minimum period before taking final weight readings. An ionizer was also used to minimize the electrostatic effect on the filter before weighing to improve the weighing accuracy. Filters were used to collect all remaining suspended particles (<0.1mm) emitted from the wind tunnel tray during testing and captured within the slot sampler that was not large enough to drop into the bottom catcher.

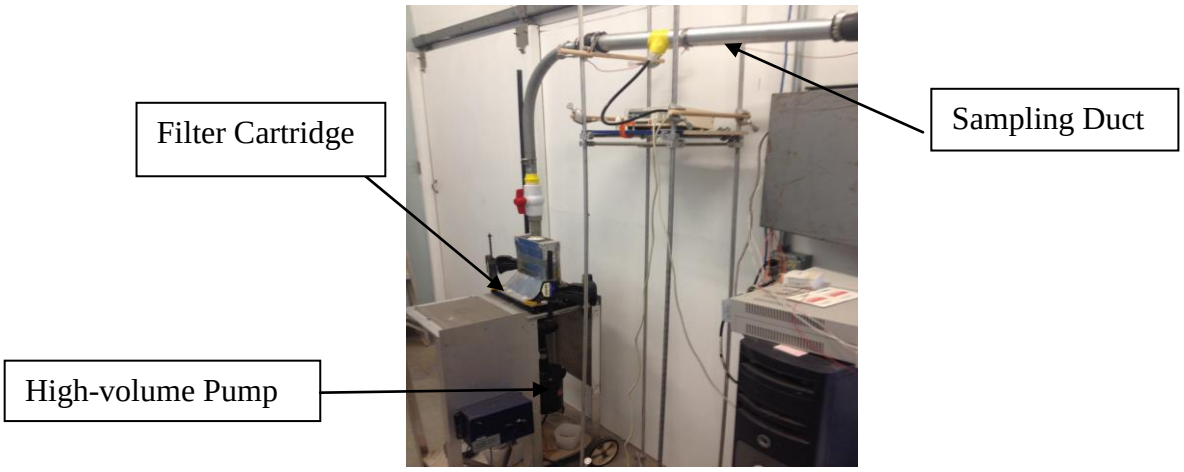

Figure 3-21. Dust sampling system

A fixed amount (7 kg) of 0.29 to 0.42 mm diameter silica sand was placed on the wind tunnel floor about 10 m upwind from the tray sample to simulate the saltating sand impacting the soil surface in an outdoor natural field condition. The same relative same shape and location

of silica sand was maintained with the use of a metal frame (Figure 3-22) for each run. After the sand abrader was placed, the metal frame was removed before testing.

Figure 3-22. Metal frame used to place sand abrader on the tunnel floor.

Before turning on the wind tunnel fan, the high-volume pump was turned on for 60 s to allow the GRIMM spectrometer to purge the sampling tube and also achieve the background particle concentration level. After 60 s, the wind tunnel fan was turned on and adjusted to achieve a wind speed of 11 m/s and left at that speed for 5 min. All the silica sand was blown downwind and most of it across the tray within this 5 min period. The suspended particles (<0.1mm) as well as creep and saltation-sized particles (0.1 to 0.84 mm) emitted from the tray surface were collected by the vertical slot sampler located immediately behind the tray (Figure 3-23). The vertical slot sampler was connected with ducting to the high-volume pump. The slot sampler consists of a cyclone insides and a catchment pan under the slot sampler. The cyclone aerodynamically separates out and deposits the larger particles into the catchment pan and lets the smaller suspended particles continue traveling through the ducting and finally collected on the filter.

After 5 min, the wind tunnel fan was turned off and the high-volume pump allowed to continue running for another 30 s to clear the sampling duct of any remaining suspended particles. Also, the duct was tapped with a wooden dowel (10 mm in diameter) to disconnect the particles sticking to the duct wall. Then, the filter was removed and placed into the humidity-controlled chamber. The particles deposited into the catchment pan were brushed into a glass jar. The wind tunnel tray was again weighed to determine the final tray weight.

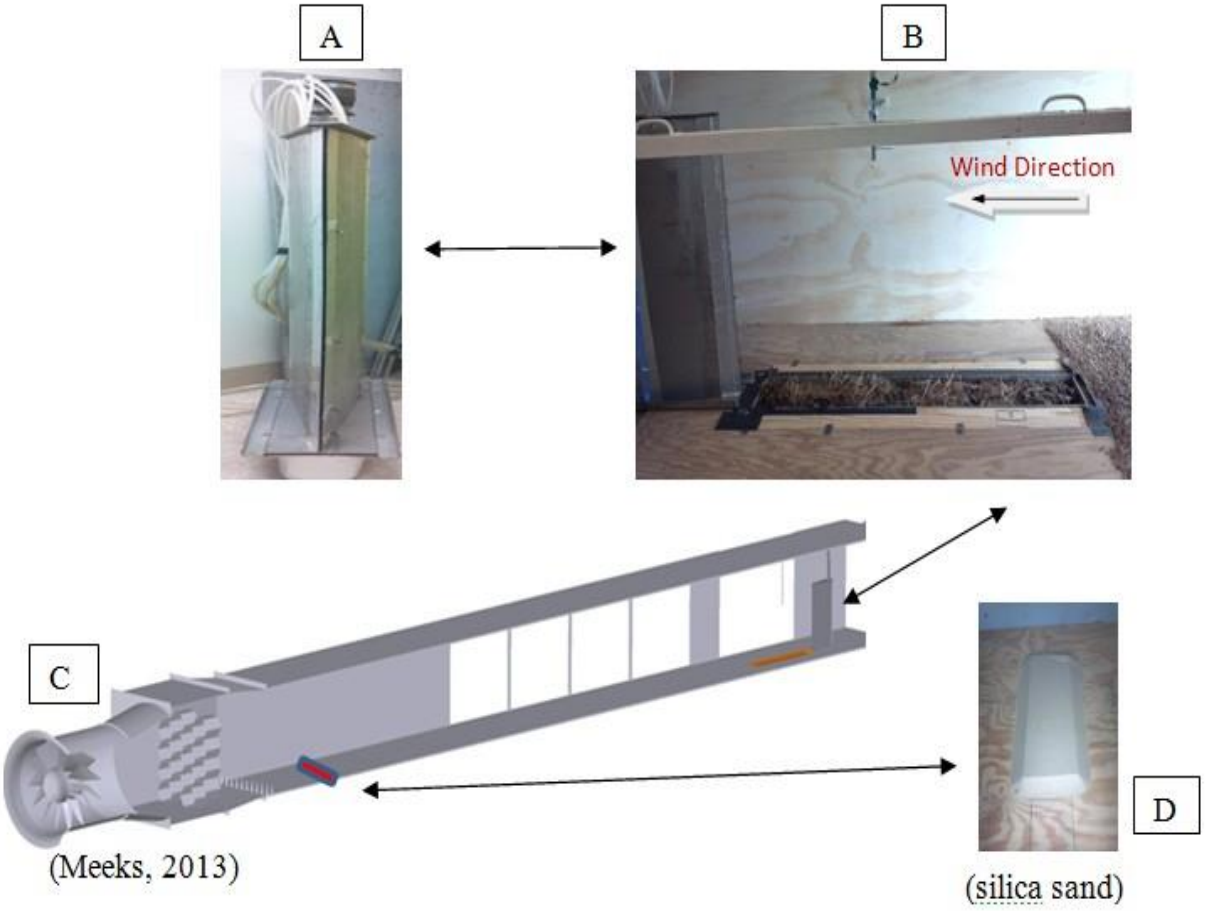

Figure 3-23. Schematic diagram of the wind tunnel setup and components: (A) slot sampler, (B) wind tunnel setup, (C) wind tunnel components, and (D) silica sand.

3.5 Data Analysis

The appropriate size bins from the GRIMM spectrometer were used to determine the concentrations of particles <2.5, <10, and <20 µm. These concentration values were then converted to emission fluxes using equation 3-2:

$$E = F * \frac{1}{\mathrm{A}} * \sum_{i=1}^{n} (C_i * \mathrm{Q}) \qquad (3\text{-}2)$$

where:

E = emission flux (mg $m^{-2}s^{-1}$)

F= unit conversion factor (0.001)

A = effective area of tray (0.0061 m^{2})

n = number of concentration measurements during the 5-min testing period

C_i = particle concentration measurements every 6 s (µg m^{-3})

Q= volumetric flowrate (m^3 s^{-1})

For each vehicle type, the emission fluxes (PM<2.5, PM<10, and PM<20) were analyzed to determine the effects of sampling location, number of vehicle passes, and soil texture.

For light-wheeled vehicles (HMMVV), the experimental design was a completely randomized design with split plot and subsampling. The soil texture (i.e., silt loam (FR), silty clay loam (FR), loamy sand (FB), sandy loam (YTC), loam (WSMR) and sandy loam (WSMR)) was the fixed whole-plot treatment factor and replication within soil was the random whole-plot error term. Split-plot fixed effects included the main effect of level of passes as minimal, moderate, and high (0, 10, 25, and 50) (Table 3-4) and the interaction between soil and the number of vehicle passes. The split-plot error term was the random effect due to the interaction between number of passes and replication within soil. For tracked vehicles (M1A1), the experimental design was exactly the same as HMMWV except the level of passes was as minimal, moderate, and high (0, 1, 5, and 10) (Table 3-5). A heavy-wheeled vehicle (M925A1) was tested at only one location and on one soil (sandy loam). Therefore, the experimental design was a randomized complete block design where the blocking factor was the replication and the treatment factor was number of passes (0, 2, 10, and 20).

Table 3-4. Light-wheeled vehicle sampling matrix.

Fort Benning					Fort Riley					Yakima Training Center					White Sands Missile Range				
Loc.**	0	10	25	50	Loc.	0	10	25	50	Loc.	0	10	25	50	Loc.	0	10	25	50
CO	●	●	●	●	CO	●*	●	●	●	CO	●	●	●	●	CO	●	●	●	●
CI	●	●	●	●	CI	●*				CI	●	●	●	●	CI	●	●	●	●
SS	●	●	●	●	SS	●*			●	SS	●	●	●	●	SS	●	●	●	●

*One initial condition sample per figure-8 replication

**Sampling locations: CO - Curve Outside, CI – Curve Inside, SS - Straight Section

Table 3-5. Tracked vehicle sampling matrix.

Fort Benning					Fort Riley					White Sands Missile Range				
Loc.**	0	1	5	10	Loc.	0	1	5	10	Loc.	0	1	5	10
CO	●	●	●	●	CO	●*	●	●	●	CO	●	●	●	●
CI	●	●	●	●	CI	●*	●	●	●	CI	●	●	●	●
SS	●	●	●	●	SS	●*	●	●	●	SS	●	●	●	●

*One initial condition sample per figure-8 replication.
**Sampling locations: CO - Curve Outside, CI – Curve Inside, SS - Straight Section.

All analyses were conducted using SAS software version 9.3 (SAS Institute Inc., 2011). Preliminary analyses assumed normality of response variables and were conducted using the Mixed procedure of SAS. However, since residuals for each of the responses appeared skewed right (i.e., non-normal), a generalized linear mixed model with a gamma distribution and a log link function in the GLIMMIX procedure of SAS were used. The selection in using a gamma distribution ensured positive dust emission confidence limits, while accounting for the heterogeneous variance experienced among soil textures. Due to unbalanced subsampling, the Satterthwaite denominator degree of freedom method was used. For the light-wheeled and tracked vehicle analyses, F-tests were calculated for the main effects of soil texture and number of passes and for soil*pass interaction. For heavy-wheeled vehicle analysis, the F-test was calculated only for the number of passes. For all analyses means and standard errors were also calculated for all effects. In addition, pairwise comparisons were performed for the main effect means using the Tukey adjustment for Type I error.

Data were also analyzed to compare the GRIMM spectrometer and filter measurements and the wind tunnel measurements (with the GRIMM spectrometer) and field measurements (PI-SWERL with DustTrak™ monitor). The PI-SWERL measurements were converted to fluxes using an effective emissive area of 0.035 m^2 (Etyemezian et al., 2007). The collected onsite data by the PI-SWERL were compared with that detected by the GRIMM spectrometer used in the non-abrader wind tunnel tests. An empirical equation relating the friction velocity to RPM was modified using a single parameter α to quantify different surface roughness:

$$U^*(RPM) = C1^* \alpha^4 * RPM^{C2/\alpha} \quad (3\text{-}3)$$

where C_1 =0.000683 and C_2= 0.832. A surface roughness lookup table was provided by Etyemezian et al. (2014) to select α value through a visual examination of surface characteristic (Table 3-6).

Table 3-6. Suggested grouping of roughness by value of α (Etyemezian et al., 2014)

Range of values of α	Roughness category
$\alpha \geq 0.96$	Use 0.98
$0.96 > \alpha \geq 0.92$	Use 0.94
$0.92 > \alpha \geq 0.88$	Use 0.90
$0.88 > \alpha \geq 0.84$	Use 0.86
$0.84 > \alpha \geq 0.80$	Use 0.82

The random roughness was calculated based on standard deviation (SD) of surface height and had been used in agriculture and wind erosion field to quantify the surface roughness, which differs from the way using a single parameter α. Therefore, an estimated equation (α= 0.806 + $0.1185e^{-SD/1.523}$) was derived to convert the random roughness to the α value (L. Hagen, personal communication). The random roughness of the wind tunnel trays ranges from 2 to 15 mm, which corresponds to the α value of 0.82. Preliminary analysis of friction velocity above wind tunnel tray surface and the friction velocity under various RPM levels indicated the 2000 rpm (corresponding to $U_* = 0.69$ m/s) of the PI-SWERL spinning blade would generate the friction velocity closest to that in the wind tunnel test (L. Hagen, personal communication). Therefore, the dust emission fluxes under the 2000 rpm were extracted to compare with the wind tunnel tray dust emission measured by the GRIMM spectrometer.

Chapter 4 - Result and Discussion

4.1 Comparison of Wind Tunnel Measurement Techniques

Wind tunnel tray dust emissions was measured by two different methods: (a) gravimetric measurement of total suspended dust collected on the glass fiber filters (referred to as the gravimetric method) and (b) light scattering technique using the GRIMM spectrometer that measured a subsample of the air stream ahead of the filters. There were no filter data collected for the wind tunnel trays at Ft. Riley as too much sand abrader was collected on the filter surface. The data presented were referred to abrader tests.

Figures 4-1 to 4-3 show strong correlation between the two methods; however, the gravimetric method measured significantly higher amount of dust than the GRIMM spectrometer. Note that the GRIMM spectrometer measures particles within the size range from 0.3μm to 20μm based on light scattering. The gravimetric method, on the other hand, collects particles of up to 100 μm or even higher. As such, the gravimetric method is expected to result in higher dust mass. Another possible explanation for the difference was the possible sampling error with the GRIMM spectrometer associated with the difficulty in maintaining isokinetic sampling conditions during the testing and possible non-uniformity in particle distribution within the sampling duct. Correlation ($R^2 = 0.98$) between these two measurement techniques was better for the WSMR samples (Figure 4-3) compared to FB (Figure 4-1) and YTC (Figure 4-2) samples ($R^2 = 0.87$ and $R^2 = 0.91$, respectively). One possible explanation is that tests for the WSMR samples used only one pump with constant flow rate, while tests for the other sites used two high-volume pumps with one being adjustable to allow flow modification to meet isokinetic conditions.

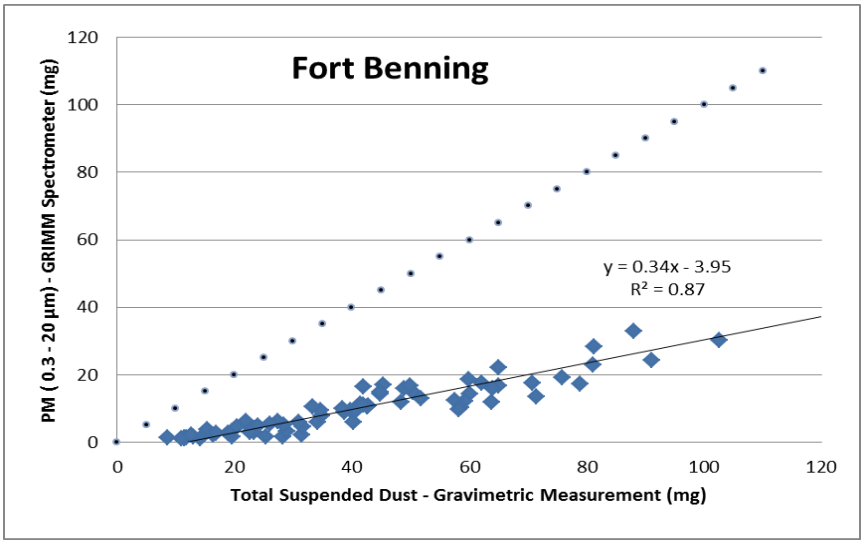

Figure 4-1. Correlation of wind tunnel abrader tests between gravimetric measurement of total suspended dust (<100 µm) and GRIMM spectrometer measurement (0.3 -20 µm) – Fort Benning (sand). The solid line represents the least-squares regression line, while the dotted line represents 1:1 correspondence.

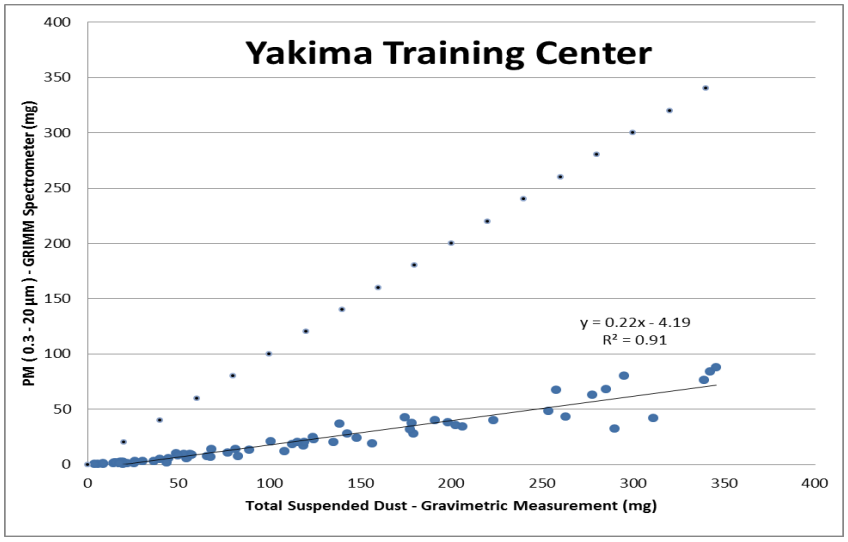

Figure 4-2. Correlation of wind tunnel abrader tests between gravimetric measurement of total suspended dust (<100 µm) and GRIMM spectrometer measurement (0.3 -20 µm) – Yakima Training Center (sandy loam). The solid line represents the least-squares regression line, while the dotted line represents 1:1 correspondence.

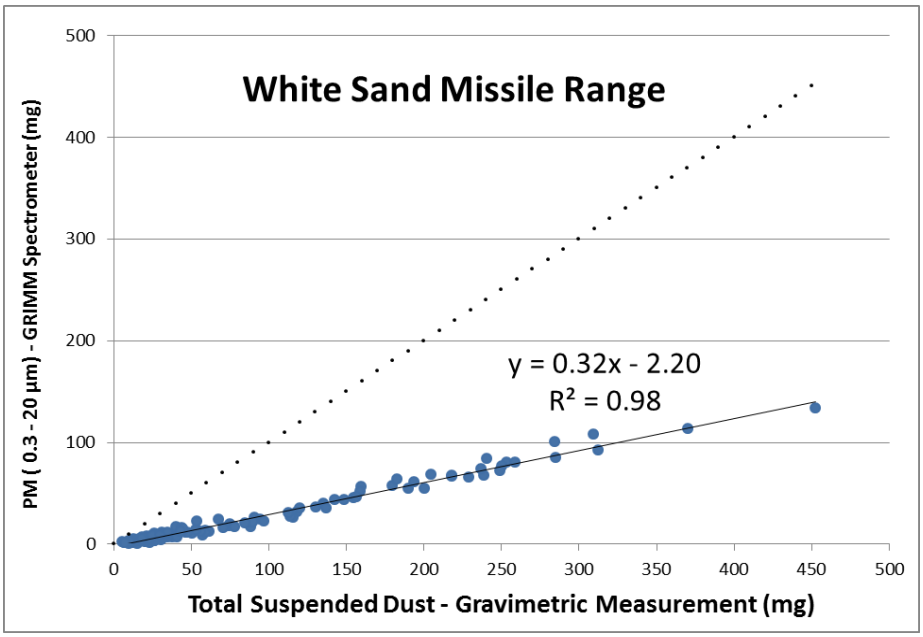

Figure 4-3. Correlation of wind tunnel abrader tests between gravimetric measurement of total suspended dust (<100 µm) and GRIMM spectrometer measurement (0.3 -20 µm) – White Sands Missile Range (loam and sandy loam). The solid line represents the least-squares regression line, while the dotted line represents 1:1 correspondence.

4.2 Effect of Sampling Period on Emission Rate

Each wind tunnel tray was tested for 5 min under a fixed amount of sand abrader (7 kg). However, the saltation flux may fluctuate during testing as the saltation flux at the beginning may reach wind transport capacity and later get lower if there was no enough abrader supply. Therefore, it was necessary to compare the different average emission rate of each wind tunnel tray among the first 3 min, first 4 min, and even all 5 min.

For the FR samples, the 4-min average emission rate of PM <10 µm was highly correlated to and close to the 5-min average emission rate as shown in Figure 4-4. The 3-min average emission rate of PM <10 µm was also strongly correlated to but larger than the 4-min average emission rate. However, the dust emission from FR tray samples was very low, therefore, the difference among various time average emission rates was relatively small. For the FB and YTC samples, the comparison between 4-min and 5-min average emission rate of PM <10 µm showed almost no difference as they were highly correlated and close to 1:1 correspondence (Figures 4-5 and 4-6). For the WSMR samples, the 4-min average emission rate

of PM <10 µm was much larger than the 5-min average emission rate as the emission value was relatively large (up to about 90 mg $m^{-2}s^{-1}$). The 3-min average emission rate of PM <10 µm, on the other hand, did not show much difference from the 4-min average emission rate (Figure 4-7). Based on the above analysis, it was determined that the 4-min average emission rate was used as an indicator of dust emission from wind tunnel tray experiments.

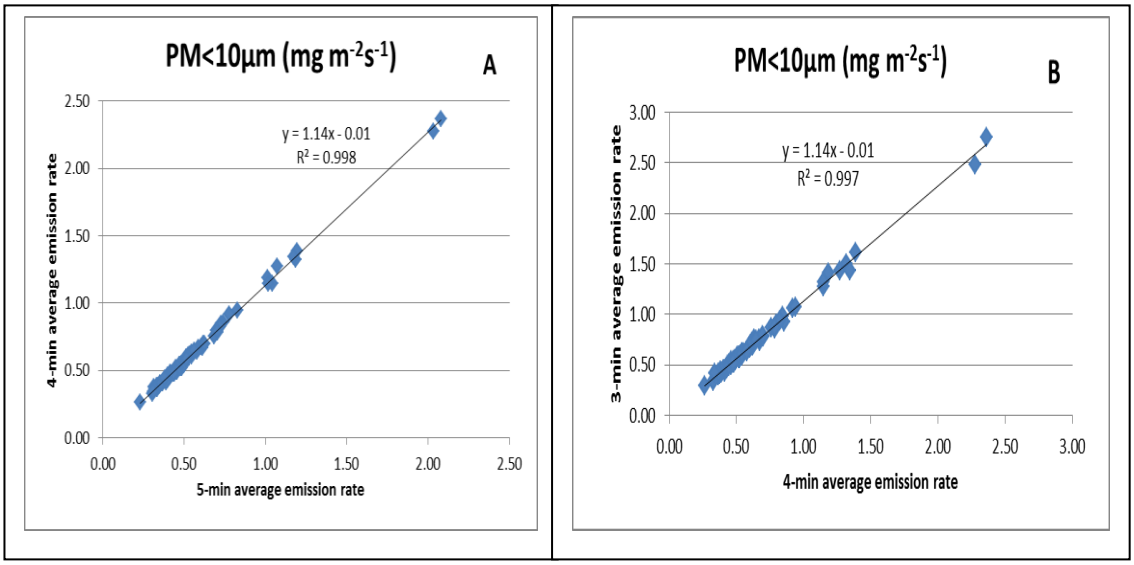

Figure 4-4. Effect of averaging time on emission rate for Fort Riley samples (silt loam and silty clay loam): (A) 4-min vs. 5-min, and (B) 3-min vs. 4-min.

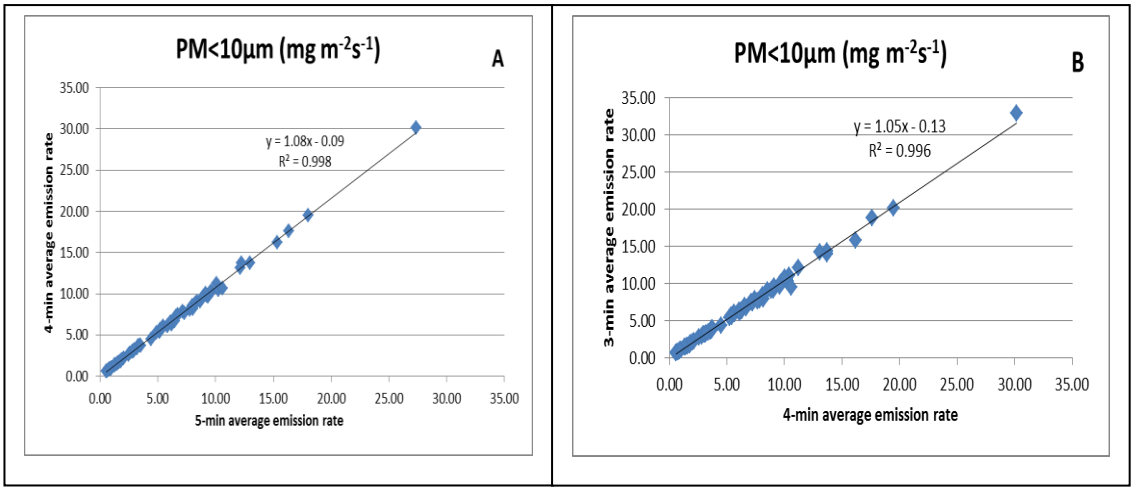

Figure 4-5. Effect of averaging time on emission rate for Fort Benning (sand): (A) 4-min vs. 5-min, and (B) 3-min vs. 4-min.

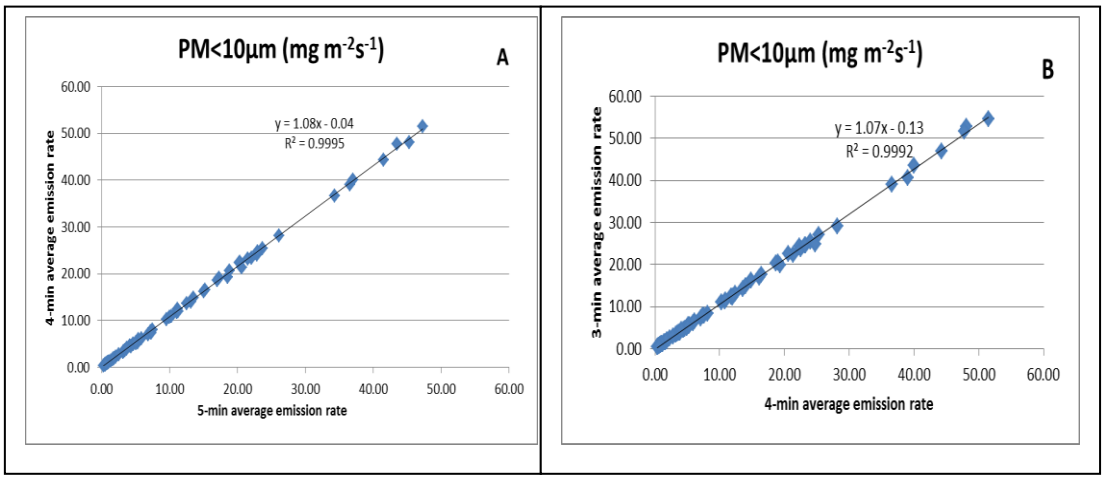

Figure 4-6. Effect of averaging time on emission rate for Yakima Training Center (sandy loam): (A) 4-min vs. 5-min, and (B) 3-min vs. 4-min.

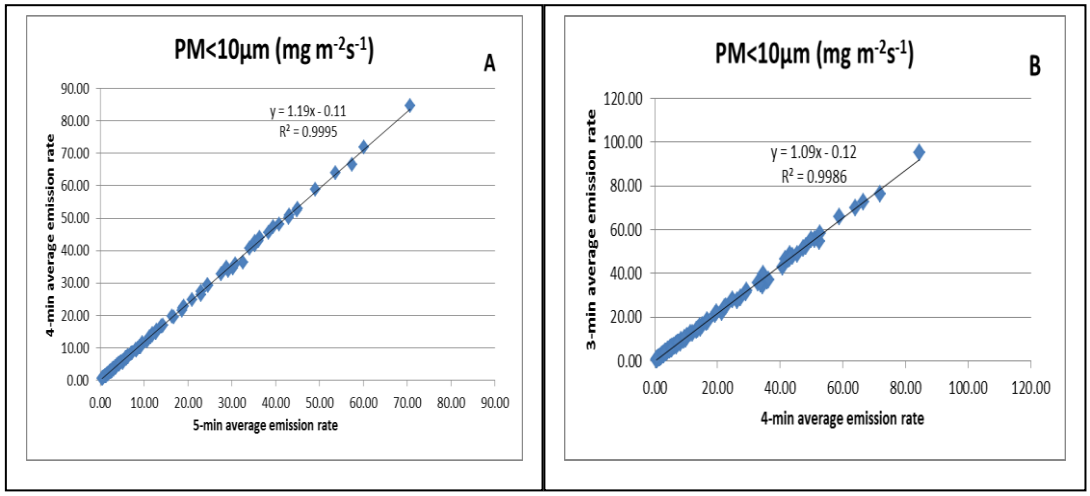

Figure 4-7. Effect of averaging time on emission rate for White Sands Missile Range (loam sand sandy loam): (A) 4-min vs. 5-min, and (B) 3-min vs. 4-min.

4.3 Laboratory Wind Tunnel Measurement –Abrader Test Results

The effect of traffic intensity (number of vehicle passes) and soil texture on dust emission potential were evaluated for each vehicle type. Dust emissions for PM<20, <10, and <2.5 µm from the GRIMM spectrometer measurement were used as dependent variable. The $PM_{2.5}/PM_{10}$ ratio ranged from 0.14 to 0.46. Figure 4-8 shows an example of wind tunnel dust emission during the testing, the concentration of PM<20 µm and PM<10 µm were close, and dust emission of PM <2.5 µm was relatively low but the trend was similar.

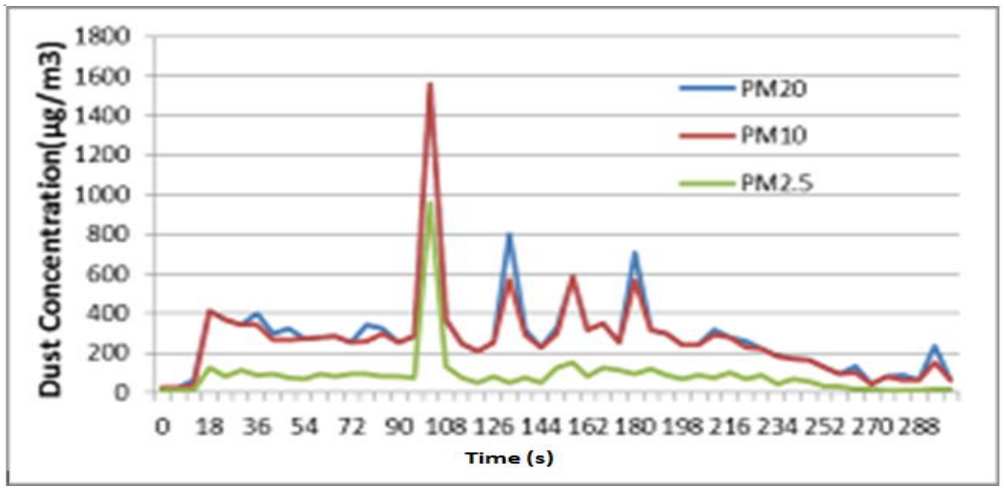

Figure 4-8. Wind tunnel tray dust emission of White Sands Missile Range at 10 passes from the straight section sampling location.

4.3.1 Light–wheeled Vehicle

Data were summarized for the light-wheeled vehicle (HMMWV) on six soil types across four experimental sites. Two soil textures were identified for testing at FR and WSMR, with only one soil texture from each of the other two sites. The soil type, vehicle passes, and sampling location three-way interaction did not show any significant effect (P>0.05). For each soil at each training site, the sampling location (i.e., SS, CO, and CI) did not show any significant effect (Table 4-1); therefore, the analysis was conducted based on average value for the three sampling locations for the light-wheeled vehicle.

Table 4-1. Type III tests of fixed effects – light-wheeled vehicle.

Effect	Numerator DF	Denominator DF	F Value	Pr > F
Pass	3	6	46.7	0.0001
Fig8Loc	2	4	0.73	0.53
Pass*Fig8Loc	6	12	0.62	0.71

No significant difference was found between silt loam soil and silt clay loam soil at FR as these two soil textures have similar sand, silt, and clay contents (Table 3-1 and Figure 4-9). No significant vehicle pass effect was found on both soils at FR.

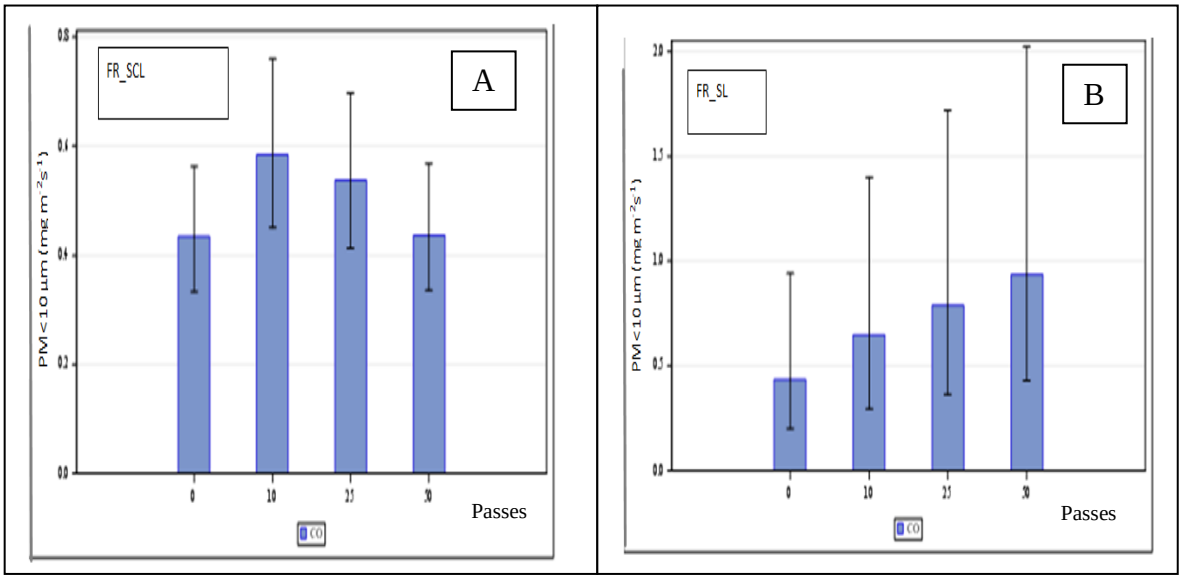

Figure 4-9. Dust emissions (PM<10 µm) from wind tunnel tests – light-wheeled vehicle: (A) silty clay loam, and (B) silt loam at Ft. Riley. Error bars represent one standard deviation.

Table 4-2 shows the pairwise comparisons for soil texture and number of passes. All but three comparisons showed significant differences at the 0.05 level. The silt loam soil at FR showed significantly (P <0.05) less emissions (PM <10 µm) than any other soil texture. This result is likely due to its low sand content but high silt and clay contents and also relatively high initial soil moisture content at FR, which assists in forming soil aggregates. There was no significant difference in emissions between sandy loam soils at YTC and at WSMR, which is not surprising as they belong to the same soil texture category. In addition, dust emission (PM <10

μm) differences between the sandy soil at FB and sandy loam soils at YTC and also WSMR were not significant (P >0.62 and P >0.71, respectively). On average, the loam soil at WSMR had the highest dust emission, whereas the silty loam soil at FR had the lowest. The loam soil had increased emission potential of 2,598% over the silt loam soil at FR.

In general, the dust emissions increased as the number of vehicle passes increased. However, it may vary from site to site. While the overall emissions at 25 passes were significantly higher than those for the 10 passes, the emission of PM<10 μm at 25 passes on the sandy loam soil at WSMR was significantly lower than at 10 passes (Figure 4-10).

The soil texture with higher sand content was more susceptible to emissions for all testing parameters. The soils (silt loam and silty clay loam) at the FR site had relatively low sand content of only 9%. While the effect of soil texture was more distinct than the vehicle passes, Table 4-3 shows evidence that the traffic intensity influenced increased emissions nearly as much as soil type alone. Figure 4-10 shows the dust emission of PM<10 μm for soil texture - number of passes interaction effects. The soils (silt loam and silty clay loam) at FR had relatively low emission potential and no obvious increasing trend compared to the other sites. Statistical analysis indicated no significant effects of vehicle passes on emissions at FR.

Table 4-3 shows the least squares means for the various treatment effects. The soils (silt loam and silty clay loam) at FR experienced increases in dust emissions from undisturbed to 25 passes, but from 25 to 50 passes, it was decreasing. One possible explanation for this is higher moisture content of the Fort Riley soils at the time of field sampling, which could aid in resisting dust emission.

Figure 4-11 shows the dust emission (PM<2.5 μm) for soil texture-number of passes interaction effects. The dust emission (PM<2.5 μm) was relatively low but showed similar trend as PM<10 μm.

Table 4-2. Pairwise comparisons of dust emission (PM <10 µm) from wind tunnel tests – light-wheeled vehicle.

Differences of Soil Least Squares Means Adjustment for Multiple Comparisons: Tukey								
Soil*	**Soil***	**Difference ($mg\ m^{-2}s^{-1}$)**	**Increase (%)**	**Standard Error**	**DF**	**t Value**	**Pr > |t|**	**Adj P**
FR_SL	FR_ SCL	-2.63	34	0.17	10	-2.75	0.0817	0.3016
FR_SL	FB_LS	-2.09	706	0.17	10	-12.08	<0.0001	<0.0001
FR_SL	YK_SaL	-2.34	934	0.17	10	-13.53	<0.0001	<0.0001
FR_SL	WS_L	-3.29	2598	0.17	10	-19.08	<0.0001	<0.0001
FR_SL	WS_SaL	-1.87	547	0.17	10	-10.81	<0.0001	<0.0001
FR_SCL	FB_LS	-2.19	694	0.17	10	-13.08	<0.0001	<0.0001
FR_SCL	YK_SaL	-2.01	913	0.17	10	-13.93	<0.0001	<0.0001
FR_SCL	WS_L	-3.29	2486	0.17	10	-19.88	<0.0001	<0.0001
FR_SCL	WS_SaL	-1.87	519	0.17	10	-11.51	<0.0001	<0.0001
FB_LS	YK_SaL	-0.25	28	0.17	10	-1.45	0.1789	0.6153
FB_LS	WS_L	-1.21	235	0.17	10	-7.00	<0.0001	0.0003
FB_LS	WS_SaL	0.22	25	0.17	10	1.27	0.2323	0.7130
YK_SaL	WS_L	-0.96	161	0.17	10	-5.55	0.0002	0.0018
YK_SaL	WS_SaL	0.47	60	0.17	10	2.72	0.0217	0.1206
WS_L	WS_SaL	1.43	317	0.17	10	8.27	<0.0001	<0.0001
Pass	**Pass**	**Difference ($mg\ m^{-2}s^{-1}$)**	**Increase (%)**	**Standard Error**	**DF**	**t Value**	**Pr > |t|**	**Adj P**
0	10	-1.38	297	0.09	30	-14.57	<0.0001	<0.0001
0	25	-1.80	503	0.09	30	-18.98	<0.0001	<0.0001
0	50	-2.28	876	0.09	30	-24.07	<0.0001	<0.0001
10	25	-0.42	52	0.09	30	-4.41	0.0001	0.0007
10	50	-0.90	146	0.09	30	-9.49	<0.0001	<0.0001
25	50	-0.48	62	0.09	30	-5.08	<0.0001	0.0001

*FR_SL(SCL) – Silt Loam and Silt Clay Loam(Fort Riley), FB_LS –Loamy Sand (Fort Benning), YK_SaL – Sandy Loam (Yakima Training Center), WS_L – Loam (White Sand Missile Range), WS_SaL – Sandy Loam (White Sand Missile Range).

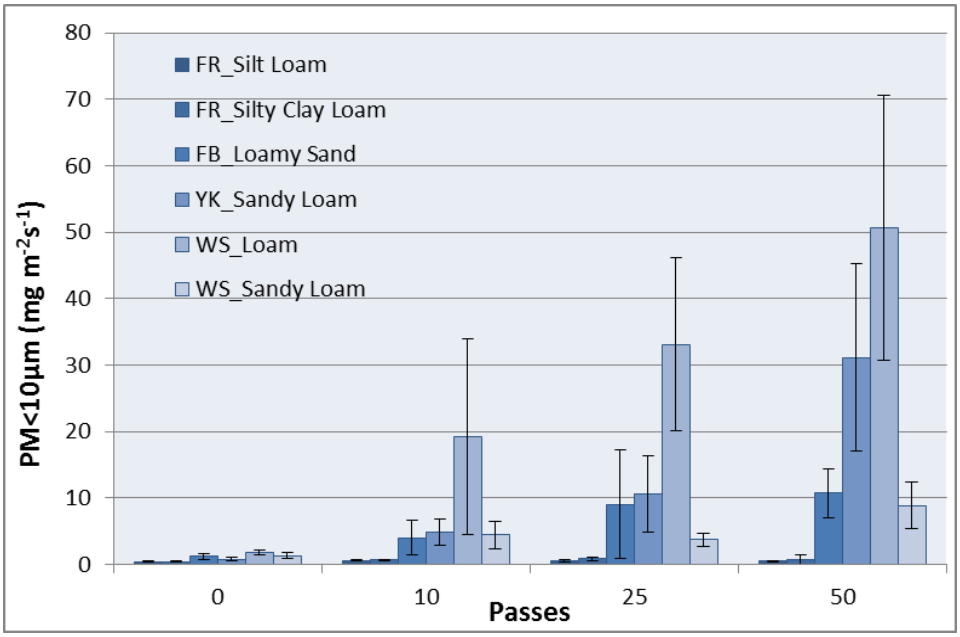

Figure 4-10. Soil-pass interaction plot for dust emissions (PM<10 µm) from wind tunnel tests– light-wheeled vehicle. Error bars represent one standard deviation.

Table 4-3. Least squares means of dust emissions from wind tunnel tests– light-wheeled vehicle.

Soil Least Squares Means			
Soil*	**PM < 20 µm**	**PM < 10 µm**	**PM < 2.5 µm**
	(mg $m^{-2}s^{-1}$)		
FR_SL	0.56	0.55	0.15
FR_SCL	0.62	0.59	0.17
FB_LS	4.69	4.58	1.29
YK_SaL	5.99	5.88	2.24
WS_L	15.77	15.34	6.36
WS_SaL	3.83	3.68	1.29
	Pass Least Squares Means		
Pass	**PM < 20 µm**	**PM < 10 µm**	**PM < 2.5 µm**
0	1.02	0.99	0.34
10	4.04	3.93	1.55
25	6.12	5.97	2.67
50	9.89	9.66	4.52

*FR_SL(SCL) – Silt Loam and Silty Clay Loam(Fort Riley), FB_LS –Loamy Sand (Fort Benning), YK_SaL – Sandy Loam (Yakima Training Center), WS_L – Loam (White Sand Missile Range), WS_SaL – Sandy Loam (White Sand Missile Range).

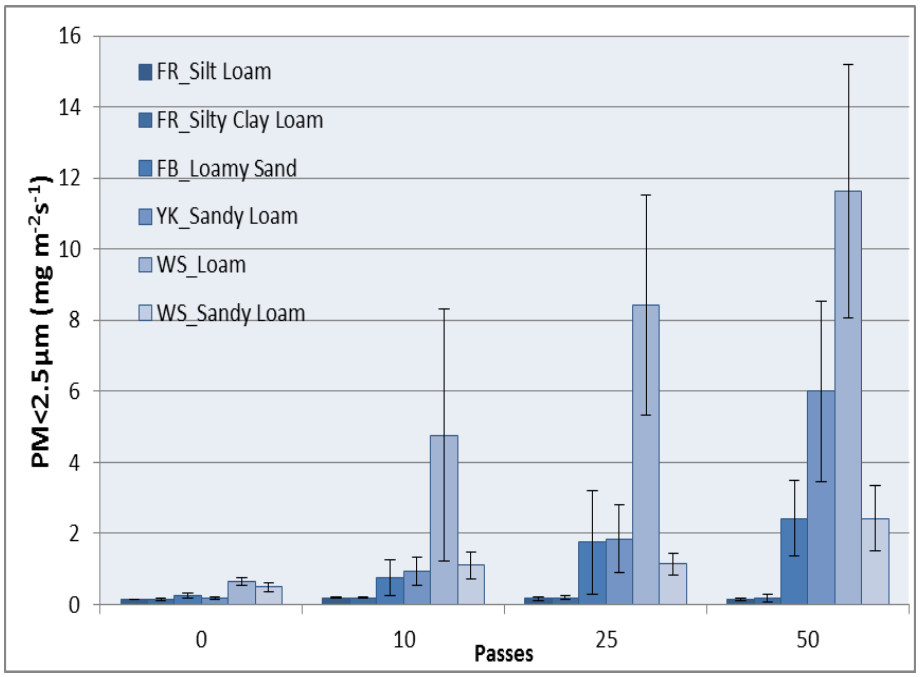

Figure 4-11. Dust emissions (PM <2.5 µm) from wind tunnel tests– light-wheeled vehicle. Error bars represent one standard deviation.

4.3.2 Tracked Vehicle

Data were summarized for the tracked vehicles on five soil textures across three sampling sites (i.e., FR, FB, WSMR). At the YTC site, a heavy-wheeled vehicle was used instead because a tracked vehicle was not available at the time of testing. The three-way interaction effect for soil type, vehicle passes, and sampling location was significant ($P<0.05$). As such, statistical analysis was conducted based on each figure 8 sampling location (i.e., SS, CI, and CO). For each sampling location, the two-way interaction effect for soil texture and passes was significant ($P<0.05$).

Table 4-4 summarizes the pairwise comparisons between soil textures. Significant differences between loamy sand soil at FB and loam soil at WSMR were found at the inside curve (CI) and outside curve (CO) sampling locations, but not at the straight section (SS) sampling location. Also, significant differences between sandy loam soil at WSMR and loam soil at WSMR were only observed at the curved section sampling locations.

Table 4-4. Pairwise comparisons of dust emissions (PM <10 µm) between soils at each sampling location - tracked vehicle.

Site_Soil	_Site_Soil	Fig8loc	Estimate	Adj P	Fig8loc	Estimate	Adj P	Fig8loc	Estimate	Adj P
FB_LS	FR_SCL	SS	2.22	<0.0001	CI	2.16	<.0001	CO	1.96	<0.0001
FB_LS	FR_SL	SS	2.03	0.0001	CI	2.25	<.0001	CO	1.80	<0.0001
FB_LS	WS_L	SS	-0.68	0.14	CI	-0.49	0.04	CO	-0.72	0.02
FB_LS	WS_SaL	SS	0.09	1.00	CI	0.10	0.95	CO	0.12	0.97
FR_SCL	FR_SL	SS	-0.19	0.94	CI	0.09	0.97	CO	-0.15	0.92
FR_SCL	WS_L	SS	-2.90	<0.0001	CI	-2.65	<.0001	CO	-2.68	<0.0001
FR_SCL	WS_SaL	SS	-2.13	<0.0001	CI	-2.05	<.0001	CO	-1.84	<0.0001
FR_SL	WS_L	SS	-2.71	<0.0001	CI	-2.74	<.0001	CO	-2.52	<0.0001
FR_SL	WS_SaL	SS	-1.93	0.0002	CI	-2.14	<.0001	CO	-1.69	<0.0001
WS_L	WS_SaL	SS	0.78	0.08	CI	0.59	0.01	CO	0.83	0.01

Table 4-5 shows pairwise comparisons of PM <10µm between number of passes at the straight section for the tracked vehicle. All the comparisons show significant differences between any two traffic intensities.

Table 4-5. Pairwise comparisons of dust emissions (PM <10 µm) between passes at the straight section (SS) sampling location - tracked vehicle.

Fig8loc	Pass	Pass	Estimate	Adj P
SS	0	1	-0.53	<0.0001
SS	0	5	-1.18	<0.0001
SS	0	10	-1.67	<0.0001
SS	1	5	-0.65	<0.0001
SS	1	10	-1.14	<0.0001
SS	5	10	-0.49	<0.0001

Figure 4-12 shows the dust emission (PM<10 µm) by tracked vehicle at the straight section (SS) for soil texture-number of passes combinations. Dust emissions (PM<10 µm) increased as the number of passes increased.

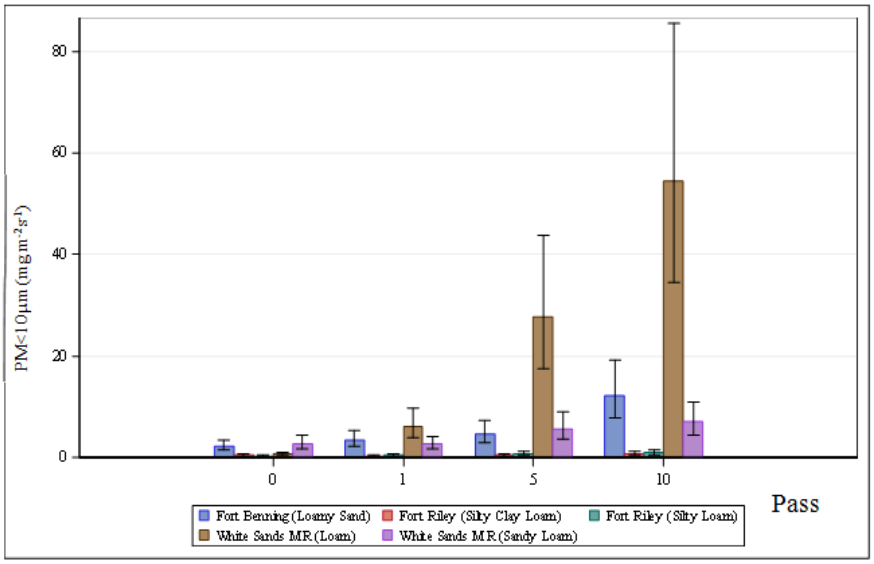

Figure 4-12. Dust emissions (PM <10 µm) at the straight section (SS) sampling location – tracked vehicle.

Table 4-6 shows pairwise comparisons of PM <10µm between number of passes at the inside curve section (CI) for the tracked vehicle. All the comparisons except one show significant differences between any two traffic intensities. No significant dust emission difference was found between 5 and 10 passes.

Table 4-6. Pairwise comparisons of dust emissions (PM <10 µm) between passes at the inside curve section (CI) sampling location - tracked vehicle.

Fig8loc	Pass	Pass	Estimate	Adj P
CI	0	1	-1.55	<0.0001
CI	0	5	-0.99	<0.0001
CI	0	10	-1.04	<0.0001
CI	1	5	0.56	0.0009
CI	1	10	0.51	0.0024
CI	5	10	-0.05	0.98

Figure 4-13 shows the dust emission (PM<10 µm) at the inside curve section (CI) for soil texture-number of passes combinations. Dust emissions under disturbed conditions were significantly higher than undisturbed conditions. The emission peak at 1 pass indicates most dust emitted at the first disturbance to soil surface.

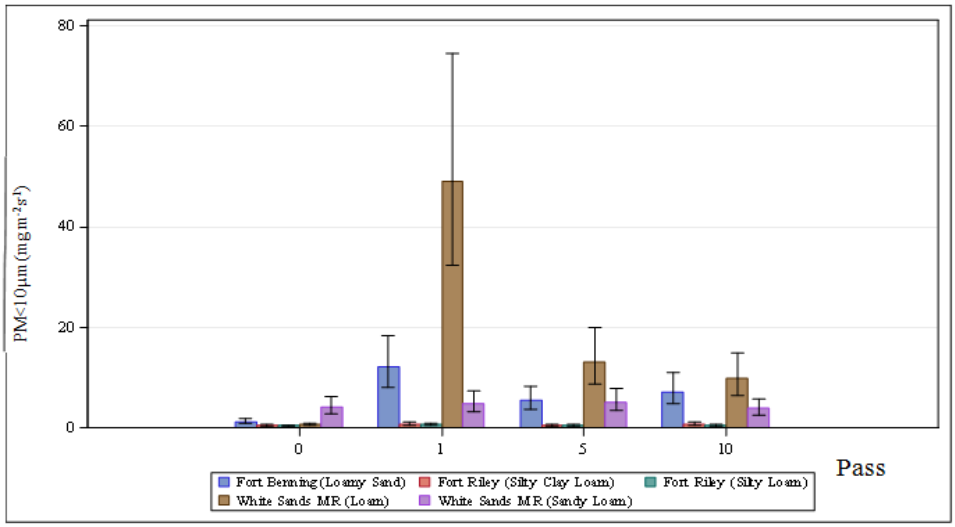

Figure 4-13. Dust emissions (PM <10 µm) at the inside curve section (CI) sampling location – tracked vehicle.

Table 4-7 shows pairwise comparisons of PM <10µm between number of passes at the outside curve section (CO) for the tracked vehicle. Significant differences in dust emissions were found between initial and disturbed conditions (P<0.05).

Table 4-7. Pairwise comparisons of dust emissions (PM<10 µm) between passes at the outside curve section (CO) sampling location - tracked vehicle.

Fig8loc	Pass	Pass	Estimate	Adj P
CO	0	1	-1.54	<0.0001
CO	0	5	-1.45	<0.0001
CO	0	10	-1.57	<0.0001
CO	1	5	0.08	0.93
CO	1	10	-0.03	0.997
CO	5	10	-0.11	0.85

Figure 4-14 shows the dust emission (PM<10 µm) by tracked vehicle at the outside curve section (CO) for soil texture-number of passes combination. Dust emissions under disturbed conditions were significantly higher than undisturbed conditions. The dust emission peak was also found at the first disturbance.

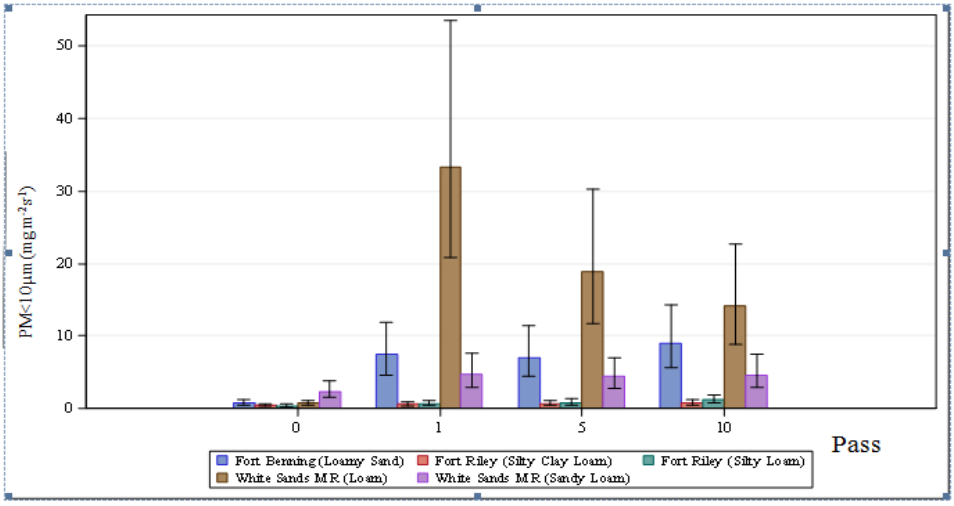

Figure 4-14. Dust emissions (PM <10 µm) at the outside curve section (CO) sampling location – tracked vehicle.

Table 4-8 shows comparisons of PM <10µm among sampling locations at FR for the tracked vehicle. Significant dust emission differences were found between the straight (SS) and curve sections (CI and CO) at 1 pass for silty clay loam soil.

Table 4-8. Dust emission (PM<10 µm) comparisons among sampling locations – tracked vehicle at Fort Riley.

Location\Pass	Initial (0)	1	5	10
FR_SCL_SS	0.44	0.38a	0.49a	0.71a
FR_SCL_CI		0.71b	0.44a	0.76a
FR_SCL_CO		0.61b	0.65a	0.77a
FR_SL_SS	0.43	0.49a	0.75a	0.91a
FR_SL_CI		0.70a	0.55a	0.51a
FR_SL_CO		0.68a	0.83a	1.23a

For a given soil texture, column means with the same letter are not significantly different at 0.05 level.

Table 4-9 shows comparisons of PM <10µm among sampling locations at FB for the tracked vehicle. Significant dust emission differences were found between the straight (SS) and outside curve (CO) sections at 0 pass and also between the straight (SS) and inside curve (CI) section for loamy sand soil.

Table 4-9. Dust emission (PM <10µm) comparisons among sampling locations – tracked vehicle at Fort Benning.

Location\Pass	0	1	5	10
FB_LM_SS	2.17a	3.45a	4.65a	12.22a
FB_LM_CI	1.23ab	12.17b	5.33a	6.90a
FB_LM_CO	0.76b	7.33ab	7.12a	8.06a

Column means with the same letter are not significantly different at the 0.05 level.

Table 4-10 shows comparisons of PM <10µm among sampling locations at WSMR for the tracked vehicle. Significant dust emission differences were found between the straight and outside curve section at 1 pass for loamy sand soil at WSMR. Significant dust emission

differences were found between the straight and inside curve section at 10 pass for loamy sand soil at WSMR. Significant dust emission differences were found between the straight and outside curve section under disturbed conditions (1, 5, and 10 passes) for loam soil at WSMR.

Table 4-10. Dust emission (PM <10µm) comparisons among sampling locations – tracked vehicle at White Sands Missile Range.

Location\Pass	0	1	5	10
WSMR_SaL_SS	2.80a	2.59a	5.70a	7.08a
WSMR_SaL_CI	4.09a	4.92b	5.12a	3.89b
WSMR_SaL_CO	2.36a	4.75b	4.39a	4.64ab
WSMR_L_SS	0.70a	6.14a	27.39a	54.40a
WSMR_L_CI	0.68a	49.01b	12.94b	9.79b
WSMR_L_CO	0.71a	33.35b	18.09b	13.91b

For a given soil texture, column means with the same letter are not significantly different at the 0.05 level.

Overall, no significant dust emission differences were found between the outside (CO) and inside curve (CI) at any pass level of any soil type. Apparently, the difference in radius between the inside and outside tracks in this study was not great enough to make any significant difference in emission results.

4.3.3 Heavy-wheeled Vehicle

Table 4-11 shows comparisons of PM <10µm (mg $m^{-2}s^{-1}$) among sampling locations at YTC for the heavy-wheeled vehicle. Similar to the light-wheeled vehicles, no significant sampling location effect was found. Therefore, analysis was conducted based on average values for the sampling locations for the heavy-wheeled vehicle. Table 4-12 shows that there were significant ($P<0.05$) treatment effects (number of passes) for all tests. After 20 passes of the heavy-wheeled vehicle, the soil surface showed 3,499% increase in dust emission potential over undisturbed conditions.

Table 4-11. Dust emission (PM <10µm) comparisons among sampling locations – heavy-wheeled vehicle at Yakima Training Center.

Location\Pass	0	2	10	20
SS	0.83a	6.93a	10.50a	21.81a
CI	0.85a	6.35a	13.53a	31.04a
CO	0.63a	3.13a	15.38a	35.89a

Column means with the same letter are not significantly different at the 0.05 level.

Table 4-12. Pairwise comparisons of dust emissions (PM <10 µm) between passes from wind tunnel tests – heavy-wheeled vehicle at Yakima Training Center.

Pass	_Pass	Difference	Increase (%)	Standard Error	DF	t Value	Pr > |t|	Adj P
0	2	-4.83	588	2.48	8	-1.95	0.087	0.28
0	10	-12.82	1560	2.48	8	-5.18	0.0008	0.0037
0	20	-28.77	3499	2.48	8	-11.62	<0.0001	<0.0001
2	10	-7.99	141	2.48	8	-3.23	0.012	0.048
2	20	-23.94	423	2.48	8	-9.67	<0.0001	<0.0001
10	20	-15.95	117	2.48	8	-6.44	0.0002	0.0009

Figure 4-15 and 4-16 show an increasing trend in dust emission potential with each subsequent increase in traffic passes for each treatment level up to 20 passes. While the light-wheeled vehicle showed less increment in emission at higher number of passes, the heavy-wheeled vehicle showed the significant increasing trend for the same soil type. However, the number of passes only went up to 20, whereas the light-wheeled vehicle used 50 passes as the upper level.

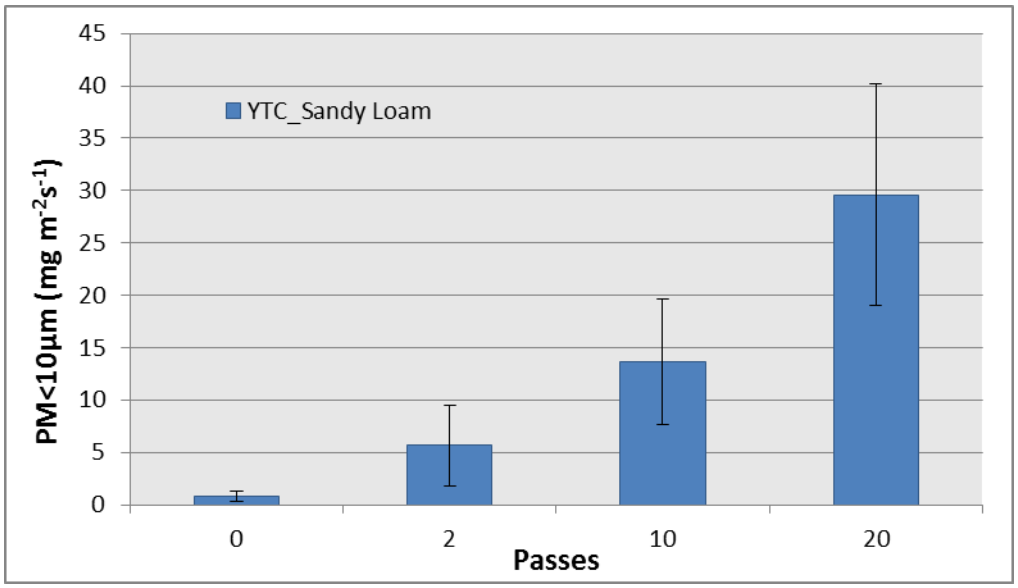

Figure 4-15. Dust emissions (PM<10 µm) by pass from wind tunnel tests – heavy-wheeled vehicle at Yakima Training Center.

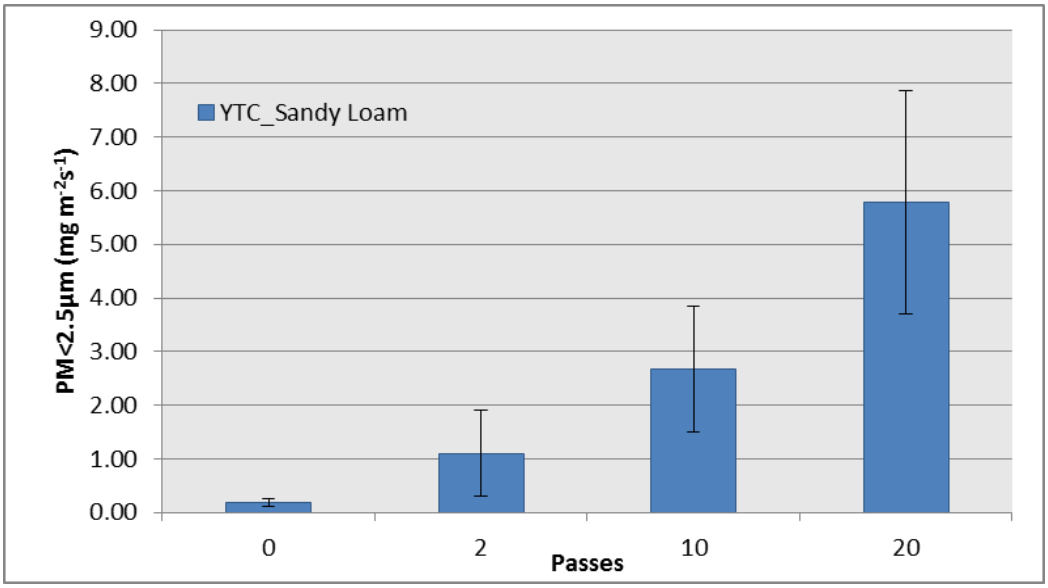

Figure 4-16. Dust emissions (PM<2.5 µm) by pass from wind tunnel tests– heavy-wheeled vehicle at Yakima Training Center.

Table 4-13 shows the least squares means of dust emission potential for the heavy-wheeled vehicles. The initial soil condition had dust (PM <10µm) emission potential of 0.82 mg $m^{-2}s^{-1}$ while a surface that had been traversed 20 times had emission potential of 29.59 mg $m^{-2}s^{-1}$

(equivalent to a 3,499% increase). The emission potential of the dust (PM < 2.5 μm) increased from 0.19 to 5.79 mg $m^{-2}s^{-1}$ (2,947%) between undisturbed conditions and 20 passes.

Table 4-13. Least squares means of dust emissions from wind tunnel tests– heavy-wheeled vehicle.

Pass	PM < 20 μm	PM < 10 μm	PM < 2.5 μm
	(mg $m^{-2}s^{-1}$)		
0	0.84	0.82	0.19
2	5.76	5.66	1.10
10	13.89	13.65	2.67
20	30.08	29.59	5.79

4.4 Aggregate Size Distribution

Aggregate size distribution has been used as an indicator for wind erosion in which aggregates <0.84 mm is considered the wind erodible fraction of soil (Hagen and Skidmore, 1976; Gillette, 1977). Soil surface samples were collected in the field and sieved by a rotary sieve to determine the aggregate <0.84 mm fraction. Table 4-14 shows the pairwise comparison for the light-wheeled vehicle. No significant (P>0.05) difference in erodible aggregates between 1, 5, and 10 passes; however, there was significant (P<0.05) difference between undisturbed and disturbed soil conditions. This can also be seen in Tables 4-15 and 4-16.

Table 4-17 shows the test of fixed effects for the aggregate size distribution for tracked vehicle. The soil texture and number of passes had significant (P<0.05) one-way effects and also the interaction was significant (P>0.05) for all vehicle types. While it is obvious that soil aggregation will vary according to soil texture, Table 4-17 shows that it is also affected by vehicle passes.

Table 4-14. Pairwise comparisons of aggregate <0.84 mm– light-wheeled vehicle.

Differences of Soil Least Squares Means Adjustment for Multiple Comparisons: Tukey								
Soil*	**Soil**	**Difference**	**Increase (%)**	**Standard Error**	**DF**	**t Value**	**Pr > |t|**	**Adj P**
FB_LS	YK_SaL	-0.35	3	0.35	17.54	-1.01	0.32	0.84
FB_LS	WS_L	0.85	12	0.32	12.16	2.67	0.02	0.12
FB_LS	WS_SaL	1.10	18	0.31	11.32	3.56	0.0043	0.029
YK_SaL	WS_L	1.20	16	0.33	14.66	3.61	0.0026	0.026
YK_SaL	WS_SaL	1.46	22	0.33	13.79	4.47	0.0005	0.0064
WS_L	WS_SaL	0.26	5	0.29	8.72	0.89	0.40	0.89
Pass	**Pass**	**Difference**	**Increase (%)**	**Standard Error**	**DF**	**t Value**	**Pr > |t|**	**Adj P**
0	10	-1.44	58	0.16	29.84	-9.19	<.0001	<.0001
0	25	-1.62	63	0.17	29.84	-9.73	<.0001	<.0001
0	50	-1.66	63	0.17	29.84	-9.68	<.0001	<.0001
10	25	-0.18	4	0.18	29.82	-1.01	0.32	0.74
10	50	-0.23	4	0.19	29.82	-1.21	0.23	0.62
25	50	-0.042	0	0.19	29.82	-0.22	0.83	0.996

*FB_LS –Loamy Sand (Fort Benning), YK_SaL – Sandy Loam (Yakima Training Center), WS_L – Loam (White Sand Missile Range), WS_SaL – Sandy Loam (White Sand Missile Range).

Table 4-15. Least squares means of aggregate <0.84 mm- light-wheeled vehicle.

Soil Least Squares Means	
Site*Soil	**Aggregate < 0.84 mm (%)**
FB_LS	91
YK_SaL	94
WS_L	81
WS_SaL	77
Pass Least Squares Means	
Pass	**Aggregate < 0.84 mm (%)**
0	52
10	82
25	85
50	85

* FB_LS –Loamy Sand (Fort Benning), YK_SaL – Sandy Loam (Yakima Training Center), WS_L – Loam (White Sand Missile Range), WS_SaL – Sandy Loam (White Sand Missile Range).

Table 4-16. Least squares means of aggregate <0.84 mm- light-wheeled vehicle.

Soil	Pass	Aggregate < 0.84 mm (%)
FB_LS	0	72
FB_LS	10	93
FB_LS	25	94
FB_LS	50	95
YK_SaL	0	78
YK_SaL	10	95
YK_SaL	25	96
YK_SaL	50	97
WS_L	0	53
WS_L	10	84
WS_L	25	87
WS_L	50	90
WS_SaL	0	69
WS_SaL	10	80
WS_SaL	25	81
WS_SaL	50	78

* FB_LS –Loamy Sand (Fort Benning), YK_SaL – Sandy Loam (Yakima Training Center), WS_L – Loam (White Sand Missile Range), WS_SaL – Sandy Loam (White Sand Missile Range).

Table 4-17. Type III tests of fixed effects for aggregate size distribution– tracked vehicle.

Effect	Numerator DF	Denominator DF	F Value	Pr > F
Soil	4	8.36	108	<.0001
Pass	3	23.9	36.9	<.0001
Soil*Pass	12	23.9	5.51	0.0004

Table 4-18 shows the pairwise comparison of the fraction of aggregates <0.84 mm. Consistent with the wind tunnel tray testing results, the soils of silt loam and silty clay loam at FR showed significantly ($P < 0.05$) less emissions (PM <10 μm) than any other soil texture. However, no significant differences were found between FB soil and WSMR which differed from the wind tunnel tray testing result. Surprisingly, there were no significant differences contained in aggregates fraction <0.84 mm between two soil textures (loam and sandy loam) at WSMR.

Similar to the wind tunnel tray testing results, significant differences between undisturbed and disturbed conditions were observed, but no significant differences among disturbed condition were found ($P > 0.05$) (Tables 4-19 and 4-20).

Table 4-18. Pairwise comparisons of aggregate percent < 0.84 mm– tracked vehicle.

Differences of Soil Least Squares Means Adjustment for Multiple Comparisons: Tukey								
Soil*	**Soil**	**Difference**	**Increase (%)**	**Standard Error**	**DF**	**t Value**	**Pr > |t|**	**Adj P**
FR_SL(SCL)	FB_LS	-3.37	260	0.20	10.5	-17.2	<.0001	<.0001
FR_SL(SCL)	WS_L	-2.16	196	0.18	7.62	-12.0	<.0001	<.0001
FR_SL(SCL)	WS_SaL	-2.19	200	0.18	7.51	-12.2	<.0001	<.0001
FB_LS	WS_L	1.21	22	0.19	9.98	6.28	<.0001	0.0009
FB_LS	WS_SaL	1.18	20	0.19	9.86	6.10	0.0001	0.0011
WS_L	WS_SaL	-0.038	1	0.18	7.02	-0.22	0.84	1.0
Pass	**Pass**	**Difference**	**Increase (%)**	**Standard Error**	**DF**	**t Value**	**Pr > |t|**	**Adj P**
0	1	-1.02	40	0.11	23.9	-8.94	<.0001	<.0001
0	5	-1.00	44	0.11	23.9	-8.69	<.0001	<.0001
0	10	-0.90	40	0.11	23.9	-8.02	<.0001	<.0001
1	5	0.019	0	0.11	23.9	0.16	0.87	1.0
1	10	0.13	3	0.11	23.9	1.09	0.29	0.70
5	10	0.10	3	0.11	23.9	0.92	0.37	0.80

*FR_SL(SCL) – Silt Loam and Silty Clay Loam(Fort Riley), FB_LS –Loamy Sand (Fort Benning), WS_L – Loam (White Sand Missile Range), WS_SaL – Sandy Loam (White Sand Missile Range).

Table 4-19. Least squares means of aggregates <0.84 mm- tracked vehicle.

Soil Least Squares Means	
Soil*	**Aggregate < 0.84 mm (%)**
FR_SL(SCL)	25
FB_LS	90
WS_L	74
WS_SaL	75
Pass Least Squares Means	
Pass	**Aggregate < 0.84 mm (%)**
0	52
1	75
5	75
10	73

*FR_SL(SCL) – Silt Loam and Silty Clay Loam(Fort Riley), FB_S – Sand (Fort Benning), WS_L – Loam (White Sand Missile Range), WS_SaL – Sandy Loam (White Sand Missile Range).

Table 4-20. Least squares means of aggregates <0.84 mm- tracked vehicle.

Soil*Pass Least Squares Means		
Soil	**Pass**	**Aggregate < 0.84 mm (%)**
FR_SL(SCL)	0	8
FR_SL(SCL)	1	35
FR_SL(SCL)	5	33
FR_SL(SCL)	10	32
FB_LS	0	83
FB_LS	1	92
FB_LS	5	93
FB_LS	10	91
WS_L	0	54
WS_L	1	79
WS_L	5	80
WS_L	10	78
WS_SaL	0	74
WS_SaL	1	77
WS_SaL	5	74
WS_SaL	10	74

4.5 Comparison of PI-SWERL and Wind Tunnel Tray Measurements

Figures 4-17 and 4-18 show the correlation of PI-SWERL (with DustTrak™ monitor) measurement and wind tunnel (with GRIMM spectrometer) test at WSMR. The R^2 value was higher for the sandy loam (R^2= 0.76) than for the loam soil (R^2= 0.56). Figure 4-19 shows an even higher correlation (R^2= 0.82) for the sandy soil at Fort Benning, which further confirmed the correlation between PI-SWERL and wind tunnel tray measurement increased as the sand content of soil increased.

While the degree of correlation was fairly high, the two methods were significantly different in measured values. One possible reason is the difference in measurement principles. Another possible reason is difference in the status of the soil surface conditions. While the PI-SWERL measurement was conducted in the field next to the location where wind tunnel trays were collected, the surfaces differed in vegetative cover and soil moisture content. Most wind tunnel tray samples were covered with at least some vegetation residue. The field measurement with the PI-SWERL may be conducted on the soil surface with different amount of vegetation covers compared to the tray sample surface. The soil moisture contents at the location where the PI-SWERL measurements were taken were likely different than those for the air dried wind tunnel tray samples after transport and storage in a greenhouse prior to testing in the wind tunnel. The threshold friction velocity increases as soil moisture increases (Chepil, 1958) as soil moisture (water bonding) helps to hold particles together (Gillette et al., 1982; Zobeck, 1991a).

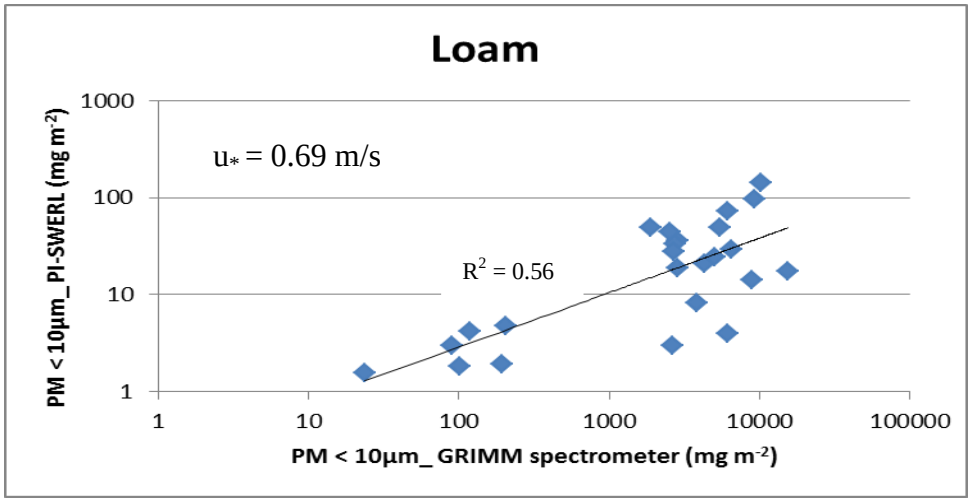

Figure 4-17. Correlation of PI-SWERL measurement and wind tunnel tray testing – loam soil at White Sands Missile Range.

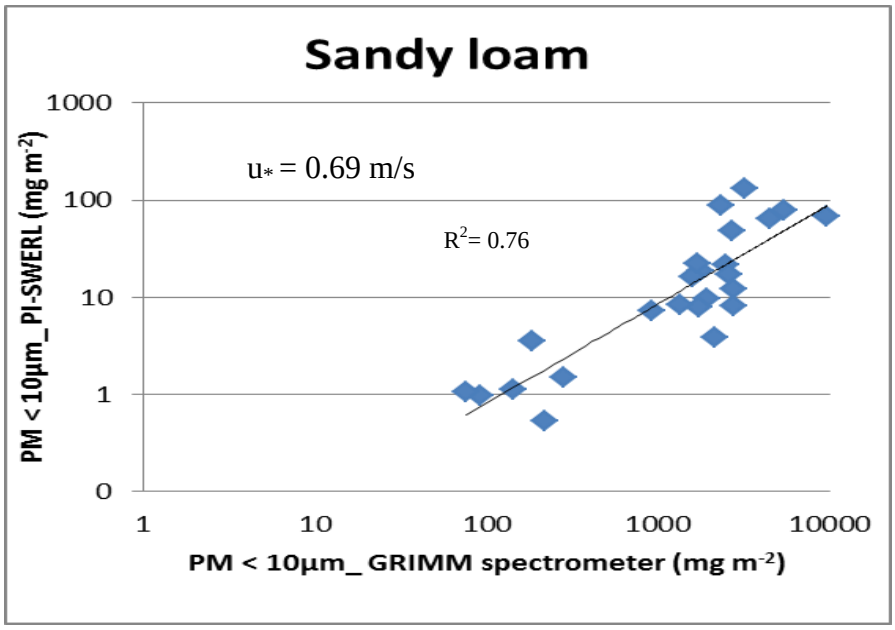

Figure 4-18. Correlation of PI-SWERL measurement and wind tunnel tray testing – sandy loam soil at White Sands Missile Range.

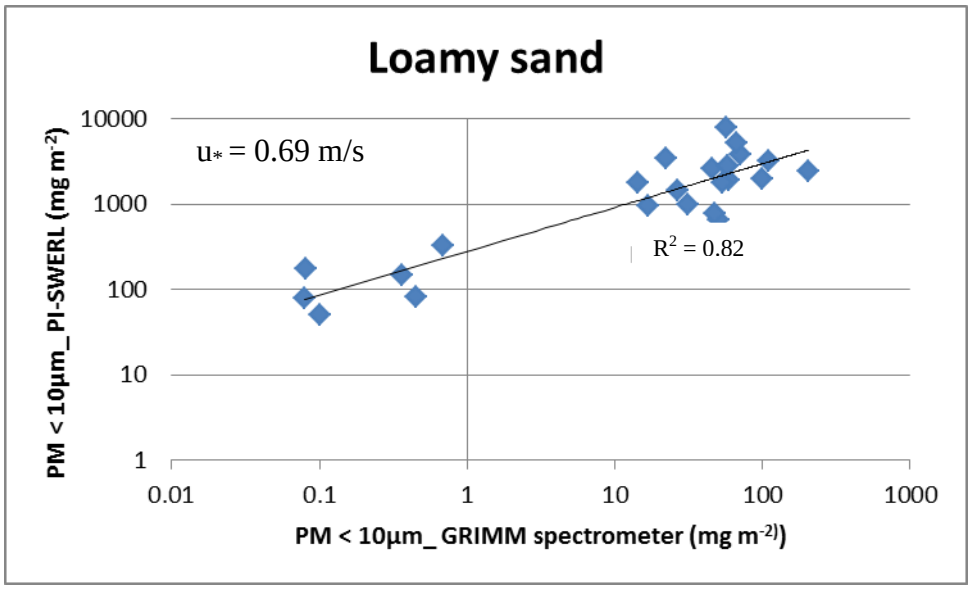

Figure 4-19. Correlation of PI-SWERL measurement and wind tunnel tray testing – loamy sand soil at Fort Benning.

4.6 Dust Entrainment Mechanisms

Table 4-21 shows the comparison of the effects of entrainment mechanism on dust emission. No significant dust differences between these two entrainment mechanisms were observed on silt loam soil at FR and Sand at FB sites (Figs 4-20 and 4-21). On the sandy loam soil at YTC and loam soil at WSMR, dust entrained by sand blasting showed significantly higher emission than aerodynamic entrainment (Figs. 4-22 and 4-23). However, the aerodynamic resuspension of loose erodible material showed significantly higher emission over the dynamic entrainment of dust for sandy loam soil at WSMR (Figure 4-24).

Table 4-21. Comparisons of PM <10 µm between wind tunnel non-abrader and abrader tests.

Differences of Least Squares Means								
Soil*	**Difference****	**Standard Error**	**DF**	**t Value**	**Pr > |t|**	**Adjustment**	**Adj P**	**α**
FR_SL	2.6	17.8	14	0.15	0.88	Tukey-Kramer	0.88	0.05
FB_S	-287.2	306.4	14	-0.94	0.36	Tukey-Kramer	0.36	0.05
YK_Sal	2223.5	485.6	14	4.58	0.0004	Tukey-Kramer	0.0004	0.05
WS_L	1707.9	582.0	16	2.93	0.0097	Tukey	0.0097	0.05
WS_SaL	-781.9	107.6	14	-7.27	<.0001	Tukey-Kramer	<.0001	0.05

*FR_SL – Silt Loam (Fort Riley), FB_S – Sand (Fort Benning), YK_SaL – Sandy Loam (Yakima Training Center), WS_L – Loam (White Sand Missile Range), WS_SaL – Sandy Loam (White Sand Missile Range).

**Difference = dynamic (abrader test) minus aerodynamic (non-abrader test) entrainment.

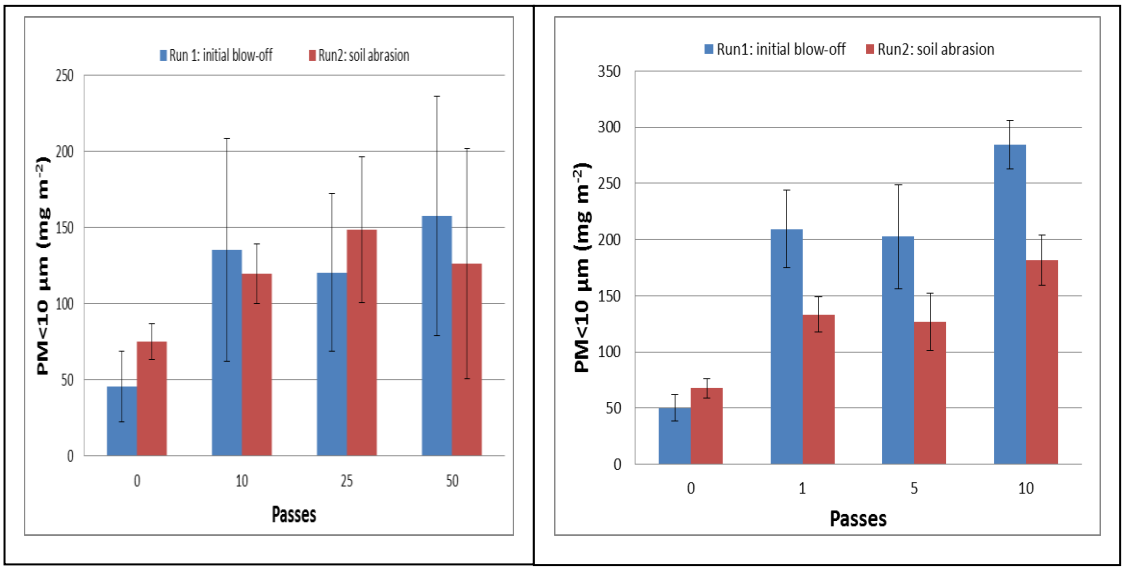

(a) **(b)**

Figure 4-20. Dust emissions (PM<10 µm) from wind tunnel tests: (a) light-wheeled vehicle and (b) tracked vehicle at Fort Riley (silty clay loam and silt loam). Error bars represent one standard deviation.

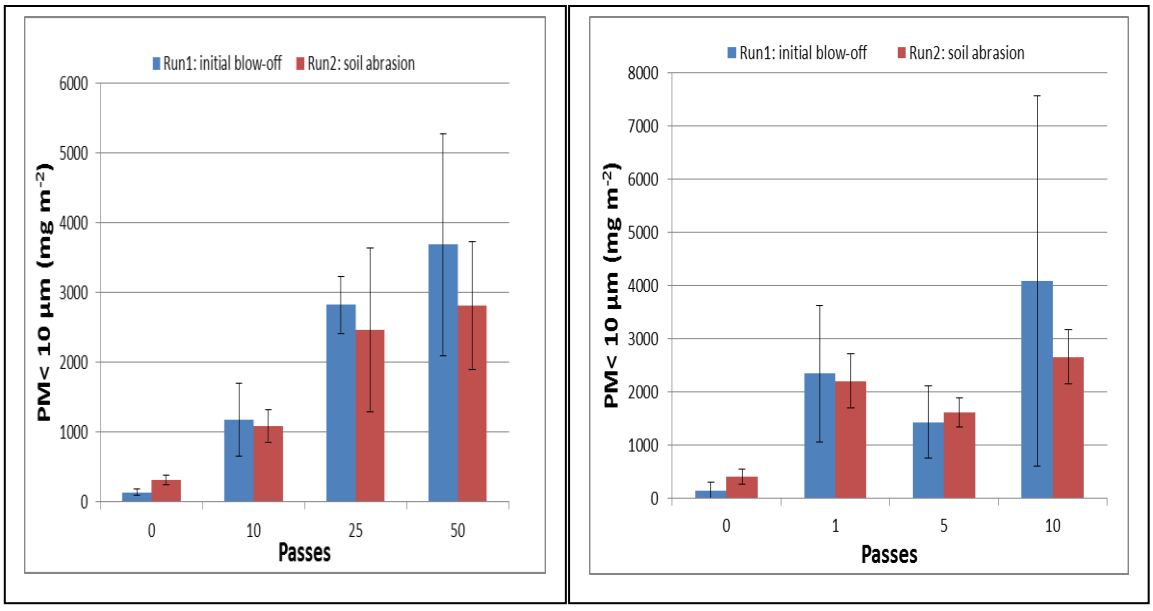

(a) **(b)**

Figure 4-21. Dust emissions (PM<10 µm) from wind tunnel tests: (a) light-wheeled vehicle and (b) tracked vehicle at Fort Benning (loamy sand). Error bars represent one standard deviation.

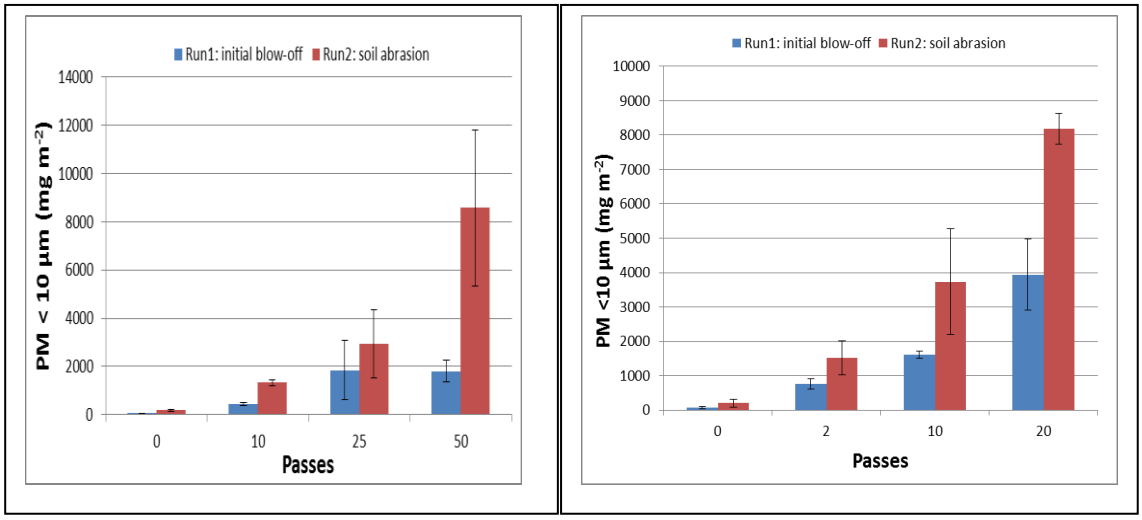

(a) **(b)**

Figure 4-22. Dust emissions (PM<10 µm) from wind tunnel tests: (a) light-wheeled vehicle and (b) heavy-wheeled vehicle at Yakima Training Center (sandy loam). Error bars represent one standard deviation.

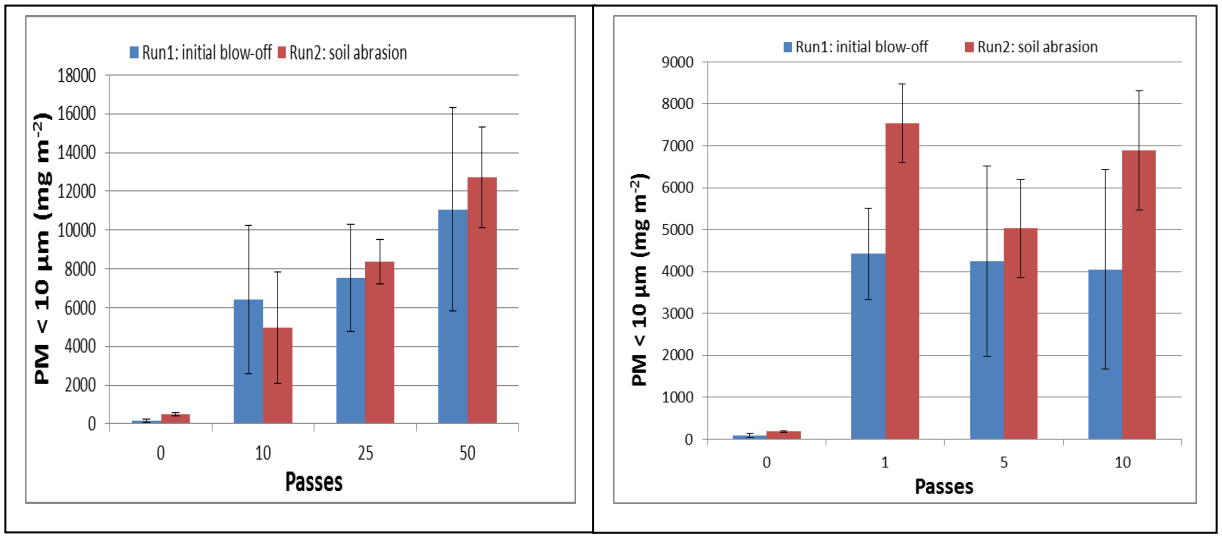

(a) **(b)**

Figure 4-23. Dust emissions (PM<10 µm) from wind tunnel tests: (a) light-wheeled vehicle and (b) tracked vehicle on loam soil at White Sands Missile Range. Error bars represent one standard deviation.

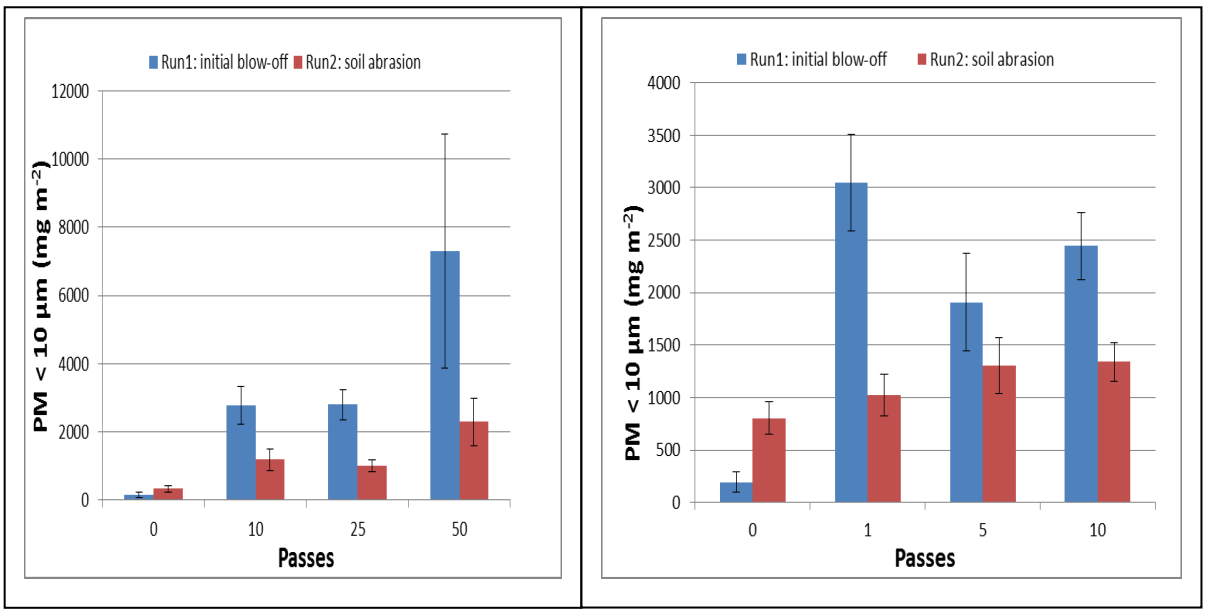

(a) **(b)**

Figure 4-24. Dust emissions (PM<10 µm) from wind tunnel tests: (a) light-wheeled vehicle and (b) tracked vehicle on sandy loam soil at White Sands Missile Range. Error bars represent one standard deviation.

4.7 Vehicle Effect

To determine the effect of vehicle type on dust emissions, the measured values from wind tunnel tests for those samples under undisturbed condition and also those under the same number of vehicle passes (10 passes) were considered. Table 4-22 shows the comparison of the effects of vehicle type on dust emission. No significant difference (P >0.05) was observed under the undisturbed condition among all sites. At 10 passes, there were significant differences in dust emission between tracked vehicle and wheeled vehicle at both FB and YTC; however, no significant differences between vehicle types were found on both two soil texture (loam and sandy loam soils) at WSMR. Figure 4-25 and 4-26 show dust emissions (PM<10 µm) among all sites. At FB and YTC, dust emissions by tracked and heavy-wheeled vehicles were much higher than that by light-wheeled vehicles as tracked vehicles weigh more than wheeled vehicles but the pressure may not. However, at WSMR, no obvious dust emission difference between two vehicle

types was observed. It is likely due to its unique soil surface characteristic, such as crusted surface presented at initial soil condition and also gravels on the soil surface.

Table 4-22. Type III tests of fixed effects for dust emissions (PM< 10 µm) for tracked and wheeled vehicles.

Site*	Soil	Pass	Vehicle	Vehicle	DF	F Value	Pr > F
FB	sand	0	tracked	wheeled	1	0.00	0.95
FB	sand	10	tracked	wheeled	1	7.75	0.024
YK	sandy loam	0	h-wheeled	wheeled	1	0.00	0.97
YK	sandy loam	10	h-wheeled	wheeled	1	27.91	0.0007
WS	loam	0	tracked	wheeled	1	0.03	0.88
WS	loam	10	tracked	wheeled	1	0.03	0.87
WS	sandy loam	0	tracked	wheeled	1	1.55	0.25
WS	sandy loam	10	tracked	wheeled	1	0.15	0.71

*FB--Fort Benning; YK-- Yakima Training Center; WS--White Sand Missile Range.

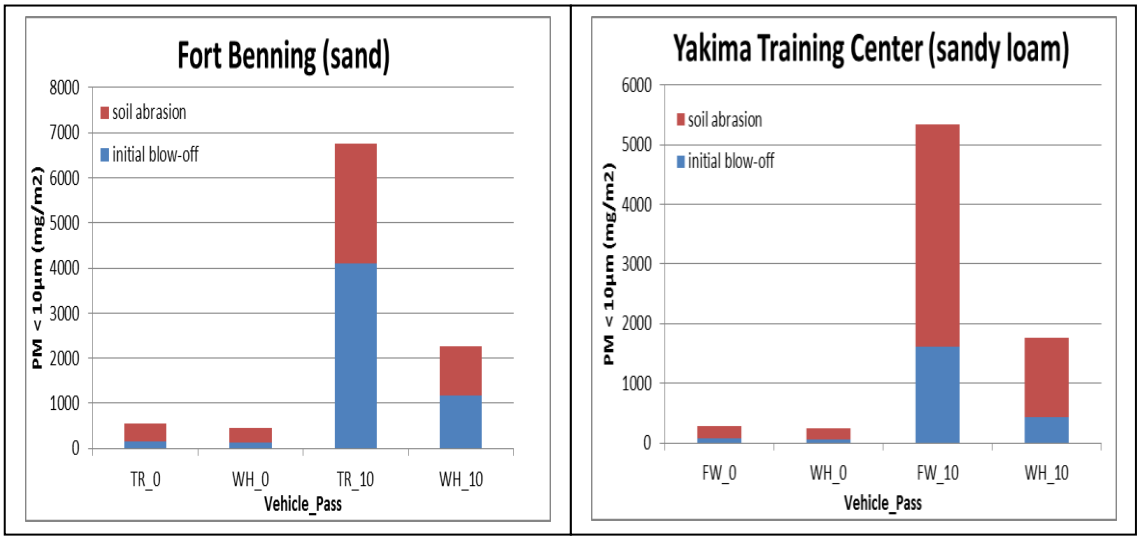

(a) (b)

Figure 4-25. Dust emissions (PM<10µm) from wind tunnel tests: (a) sandy soil at Fort Benning; and (b) sandy loam soil at Yakima Training Center.

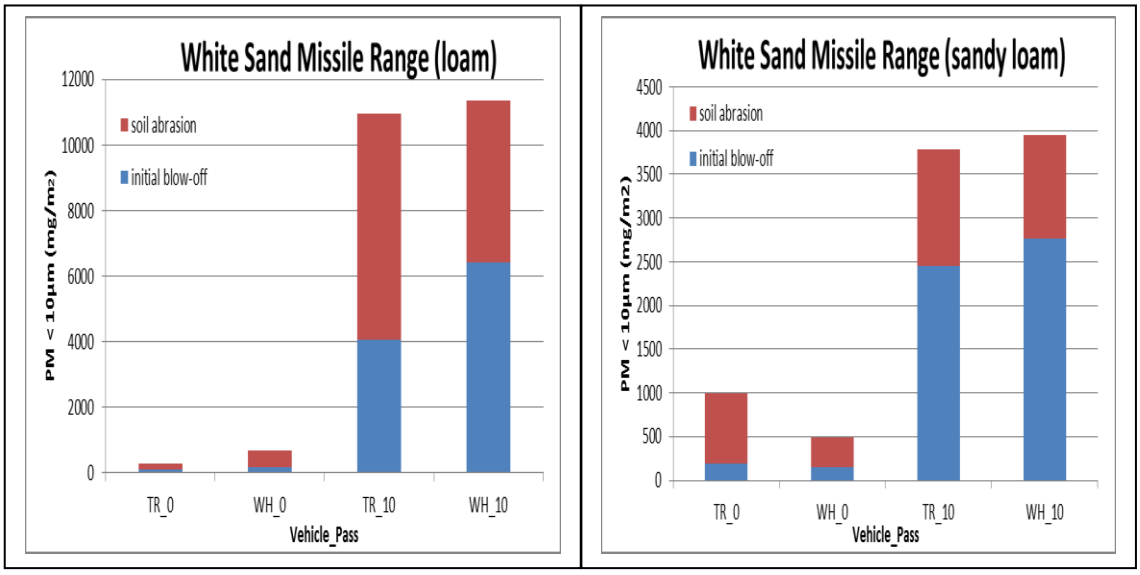

(a) (b)

Figure 4-26. Dust emissions (PM<10µm) from wind tunnel tests: (a) loam soil; and (b) sandy loam soil at White Sands Missile Range.

Chapter 5 - Conclusions

Multi-pass off-road traffic experiments involving military wheeled and tracked vehicles were conducted on six soil textures across four military training installations. Dust emission potential was measured on site by the PI-SWERL equipped with a DustTrak™ dust monitor. Soil samples at three sampling locations were also collected and tested in a laboratory wind tunnel (with sand abrader) for dust emission potential using a GRIMM aerosol spectrometer and gravimetric method with filters. The dust emissions (PM <20μm, 10μm, and <2.5 μm) from the GRIMM spectrometer measurements were selected as the primary response variable. The following conclusions were drawn from this study:

(1) Comparison of the PI-SWERL (with DustTrak™ dust monitor) and wind tunnel (with GRIMM aerosol spectrometer) measurement results showed that the two methods differed significantly in measured values but were linearly related depending on the type of soil.

(2) The gravimetric and GRIMM spectrometer data from the wind tunnel tests were also significantly different but highly correlated ($R^2 \geq 0.87$).

(3) For the light-wheeled and heavy-wheeled vehicles, wind tunnel test results (with sand abrader) showed no significant effects of sampling locations (straight section, curve inside, curve outside). Results also showed positive relationship between number of vehicle passes and dust emissions for the light-wheeled and heavy-wheeled vehicles. From undisturbed conditions to 10 vehicle passes, there was a significant ($P<0.05$) increase in dust emissions (297%) on average for all light-wheeled vehicle tests. From 10 to 25 passes and 25 to 50 passes, an additional 52% and 62%, respectively increments were observed.

(4) For the tracked vehicle, wind tunnel test results showed significant difference between the straight section sampling location and the curve section sampling locations. Also, for the straight section sampling location, dust emission increased as the number of passes increased. For the curve section sampling locations, dust emissions at any level of pass were significantly higher than initial condition; beyond first pass, no significant increase was observed.

References

Alfaro, S. C., J. L. Rajot, and W. Nickling. 2004. Estimation of PM20 emissions by wind erosion: main sources of uncertainties. *Geomorphology*, 59(1): 63-74.

Allmaras, R.R., R.E. Burwell, W.E. Larson, and R.F. Holt. 1966. Total porosity random roughness of the interrow zone as influenced by tillage. USDA Conserv. Res. Rep. 7. Washington, DC:GPO.

Althoff, P. S., S. J. Thien, and T. C. Todd. 2010. Primary and residual effects of Abrams tank traffic on prairie soil properties. *Soil Science Society of America Journal*, 74(6): 2151–2161. doi:10.2136/sssaj2009.0091

Armbrust, D. V. 1982. Physiological responses to wind and sandblast damage by grain sorghum plants. *Agronomy Journal*, 74(1): 133-135.

Ayers, P. D. 1994. Environmental damage from tracked vehicle operation. *Journal of Terramechanics*, 31(3): 173-183.

Bacon, S. N., E. V. McDonald, R. Amit, Y. Enzel, and O. Crouvi . 2011. Total suspended particulate matter emissions at high friction velocities from desert landforms. *Journal of Geophysical Research: Earth Surface*,116, F03019, doi:10.1029/2011JF001965.

Baddock, M. C., T. M. Zobeck, R. S. Van Pelt, and E. L. Fredrickson. 2011. Dust emissions from undisturbed and disturbed, crusted playa surfaces: Cattle trampling effects. *Aeolian Research*, *3*(1): 31-41.

Bagnold R. A. 1941. The Physics of Blown Sand and Desert Dunes. Methuen, London.

Belnap, J. 1995. Surface disturbances: their role in accelerating desertification. In *Desertification in Developed Countries* (pp. 39-57). Springer Netherlands.

Belnap, J., and D. A. Gillette. 1997. Disturbance of biological soil crusts: impacts on potential wind erodibility of sandy desert soils in southeastern Utah. *Land Degradation and Development*, *8*(4): 355-362.

Belnap, J., and D. A. Gillette. 1998. Vulnerability of desert biological soil crusts to wind erosion: the influences of crust development, soil texture, and disturbance. *Journal of Arid Environments*, *39*(2): 133-142.

Belnap, J., S. L. Phillips, J. E. Herrick, and J. R. Johansen. 2007. Wind erodibility of soils at Fort Irwin, California (Mojave Desert), USA, before and after trampling disturbance: implications for land management. *Earth Surface Processes and Landforms*, *32*(1): 75-84.

Braunack M.V. 1986. The residual effects of tracked vehicles on soil surface properties. *Journal of Terramechanics*, 23(1): 141-151.

Chepil, W.S. 1958. Soil conditions that influence wind erosion. USDA Technical Bulletin 1185. U.S. Government Printing Office, Washington, D.C.

Chepil, W. S. and N.P. Woodruff. 1963. The physics of wind erosion and its control. *Advances in Agronomy*, 15: 1-3-1. Academic Press, New York.

Chepil, W.S., F.H. Siddoway, D.W. Fryrear, and D.V. Armbrust. 1963. Vegetative and non vegetative materials to control wind erosion. *Soil Science Society of America Journal*, 27, 29–33.

Diersing, V. E., and W. D. Severinghaus. 1984.The Effects of Tactical Vehicle Training on the Lands of Fort Carson, Colorado. *An Ecological Assessment*. No. CERL-TR-N-85/03. Construction Engineering Research Lab, Champaign, IL.

Eames, I., and S. B. Dalziel. 2000. Dust resuspension by the flow around an impacting sphere. *Journal of Fluid Mechanics*, 403: 305-328.

Etyemezian, V., G. Nikolich, S. Ahonen, M. Pitchford, M. Sweeney, R. Purcell, J. Gillies, and H. Kuhns. 2007. The Portable In Situ Wind Erosion Laboratory (PI-SWERL): A new method to measure PM_{10} windblown dust properties and potential for emissions. *Atmospheric Environment*, 41(18): 3789–3796. doi:10.1016/j.atmosenv.2007.01.018

Etyemezian, V., J. A. Gillies, M. Shinoda, G. Nikolich, J. King, and A. R. Bardis. 2014. Accounting for surface roughness on measurements conducted with PI-SWERL: Evaluation of a subjective visual approach and a photogrammetric technique. *Aeolian Research*, 13:35-50.

Funk, R., H. I. Reuter, C. Hoffmann, W. Engel, and D. Öttl. 2008. Effect of moisture on fine dust emission from tillage operations on agricultural soils. *Earth Surface Processes and Landforms*, 33(12): 1851-1863.

Gee, G.W., and O. Dani 2002. Particle-size Analysis. In Dane, J.H. and Topp, G.C., eds., *Methods of Soil Analysis: Part 4, Physical Methods* Book Series No. 5, Madison, Wisconsin, Soil Science Society of America.

Gillette, D.A. 1977. Fine particulate emissions due to wind erosion. *Transactions of ASAE*, 20(5): 890-897.

Gillette, D. A. 1981. Production of dust that may be carried great distances. *Geological Society of America Special Papers*, 186: 11-26.

Gillette, D.A., J. Adams, D. Kuhs, and R. Kihl. 1982. Threshold friction velocities and rupture moduli for crusted deserted soils for the input of soil particles into the air. *Journal of Geophysical Research,* 87: 9003-9015.

Gillette, D. A., T. C. Niemeyer, and P. J. Helm. 2001. Supply-limited horizontal sand drift at an ephemerally crusted, unvegetated saline playa. *Journal of Geophysical Research: Atmospheres (1984–2012)*, 106(D16): 18085-18098.

Gillies, J. A., V. Etyemezian, H. Kuhns, D. Nikolic, and D. A. Gillette. 2005. Effect of vehicle characteristics on unpaved road dust emissions. *Atmospheric Environment*, 39(13): 2341-2347.

Goossens, D. 2004. Effect of soil crusting on the emission and transport of wind-eroded sediment: field measurements on loamy sandy soil. *Geomorphology*, 58(1): 145-160.

Goossens, D., and B. Buck. 2009. Dust dynamics in off-road vehicle trails: measurements on 16 arid soil types, Nevada, USA. *Journal of Environmental Management*, 90(11): 3458-3469.

Goran WD, L.L. Radke, and W.D Severinghaus. 1983. An overview of the ecological effects of tracked vehicles on major US Army Installations. United Sates Army Corps of Engineers, Construction Engineering Research Laboratory, Technical Report N-142.

Grantham, W. P., E. F. Redente, C. F. Bagley, and M. W. Paschke. 2001. Tracked vehicle impacts to vegetation structure and soil erodibility. *Journal of Range Management*, 54(6): 711-716.

Green, L. C., and S. R. Armstrong. 2003. Particulate matter in ambient air and mortality: toxicologic perspectives. *Regulatory Toxicology and Pharmacology*, 38(3): 326-335.

Hagen, L. J. 1991. Wind erosion mechanics. Abrasion of aggregated soil. *Transactions of the ASAE*, 34(4): 831-837.

Hagen, L. 1999. Assessment of wind erosion parameters using wind tunnels. Sustaining the Global Farm. (pp. 742–746). D. E. Stott, R. H. Mohtar and G. C. Steinhardt (Eds.). West Lafayette, IN: International Soil Conservation Organization. Retrieved from: http://www.tucson.ars.ag.gov/isco/isco10/SustainingTheGlobalFarm/P003-Hagen.pdf

Hagen, L.J. 2004a. Evaluation of the Wind Erosion Prediction System (WEPS) erosion submodel on cropland fields. *Environmental Modelling Software*. 19 (2): 171-176.

Hagen, L. 2004b. Fine particulates (PM10 and PM2.5) generated by breakage of mobile aggregates during simulated wind erosion. *Transactions of the ASABE*, 47(1): 107-112.

Hagen, L. J. ,and E. L. Skidmore. 1977. Wind erosion and visibility problems. *Transactions of the ASAE*, 20(5): 898-903.

Hagen, L., N. Mirzamostafa, and A. Hawkins. 1996. PM-10 generation by wind erosion. International Conference on Air Pollution from Agricultural Operations Proceedings. Midwest Plan Service, Ames, IA.

Hagen, L.J, L.E. Wagner, and E.L. Skidmore. 1999. Analytical solutions and sensitivity analyses for sediment transport in WEPS. *Transactions of the ASABE,* 42(6):1715-1721.

Hagen, L. J., and N. P. Woodruff. 1973. Air pollution from duststorms in the Great Plains. *Atmospheric Environment*, 7(3): 323-332.

Horn, R., P. S. Blackwell, and R. White. 1989.The effect of speed of wheeling on soil stresses, rut depth and soil physical properties in an ameliorated transitional red-brown earth. *Soil and Tillage Research*, 13(4): 353-364.

Houser, C. A., and W. G. Nickling. 2001a. The emission and vertical flux of particulate matter< 10 μm from a disturbed clay-crusted surface. *Sedimentology*, 48(2): 255-267.

Houser, C. A. and W. G. Nickling. 2001b. The factors influencing the abrasion efficiency of saltating grains on a clay-crusted playa. *Earth Surface Processes and Landforms*, 26(5): 491-505.

Kavouras, I. G., V. Etyemezian, G. Nikolich, J. Gillies, M. Sweeney, M. Young, and D. Shafer. 2009. A new technique for characterizing the efficacy of fugitive dust suppressants. *Journal of Air and Waste Management Association*, 59(5): 603-612.

Kjelgaard, J., B. Sharratt, I. Sundram, B. Lamb, C. Claiborn, K. Saxton, and D. Chandler. 2004. PM_{10} emission from agricultural soils on the Columbia Plateau: comparison of dynamic and time-integrated field-scale measurements and entrainment mechanisms. *Agricultural and Forest Meteorology*, 125(3): 259-277.

Kohake, D. J., L. J. Hagen, and E. L. Skidmore. 2010. Wind erodibility of organic soils. *Soil Science Society of America Journal*, 74(1): 250–257. doi:10.2136/sssaj2009.0163

Laflen, J. M., M. Amemiya, and E. A. Hintz. 1981. Measuring crop residue cover. *Journal of Soil and Water Conservation*, 36(6): 341-343.

Lee, J. A., and V. P. Tchakerian. 1995. Magnitude and frequency of blowing dust on the Southern High Plains of the United States, 1947–1989. *Annals of the Association of American Geographers*, 85(4): 684-693.

Loosmore, G. A., and J. R. Hunt. 2000. Dust resuspension without saltation. *Journal of Geophysical Research: Atmospheres (1984–2012)*, 105(D16), 20663-20671

Lyles, L., J. Dickerson, and L. Disrud. 1970. Modified rotary sieve for improved accuracy. *Soil Science*, 109(3): 207–210. Retrieved from:

http://journals.lww.com/soilsci/Abstract/1970/03000/Modified_Rotary_Sieve_for_Improved_Accuracy.11.aspx

Lyles, L. 1975. Possible effects of wind erosion on soil productivity. *Journal of Soil and Water Conservation*, 30:279-283.

Macpherson, T., W. G. Nickling, J. A. Gillies, and V. Etyemezian. 2008. Dust emissions from undisturbed and disturbed supply-limited desert surfaces. *Journal of Geophysical Research: Earth Surface*, 113, F02S04, doi:10.1029/2007JF000800.

Meeks, J. C. 2013. Fugitive dust emissions from off-road vehicle maneuvers on military training lands. M.S. Thesis. Kansas State University.

Mirzamostafa, N., L. R. Stone, L. J. Hagen, and E. L. Skidmore. 1998. Soil aggregate and texture effects on suspension components from wind erosion. *Soil Science Society of America Journal*, 62(5): 1351-1361.

NASA. 2010. *Pitot-static tube*. Retrieved from: http://www.grc.nasa.gov/WWW/k-12/airplane/pitot.html

Nickling, W. G. and J. A. Gillies.1989. Emission of fine-grained particulates from desert soils. *Paleoclimatology and Paleometeorology: modern and past patterns of global atmospheric transport* (pp. 133-165). Springer Netherlands.

Padgett, P. E., D. Meadows, E. Eubanks, and W. E. Ryan. 2008. Monitoring fugitive dust emissions from off-highway vehicles traveling on unpaved roads and trails using passive samplers. *Environmental Monitoring and Assessment*, 144(1-3): 93-103.

Pope III, C. A., M. J. Thun, M. M. Namboodiri, D. W. Dockery, J. S. Evans, F. E. Speizer, and C. W. Heath Jr. 1995. Particulate air pollution as a predictor of mortality in a prospective study of US adults. *American Journal of Respiratory and Critical Care Medicine*, 151(3): 669-674.

Presley, D., and J. Tatarko. 2009. Principles of wind erosion and its control. MF-2860. Kansas State University Research and Extension, Manhattan, KS.

Radforth J.R. 1973. Long term effects of summer traffic by tracked vehicles on tundra. Task Force on Northern Oil Development Report No. 73-22.

Ravi, S., P. D'Odorico, T. M. Over, and T. M. Zobeck. 2004. On the effect of air humidity on soil susceptibility to wind erosion: The case of air-dry soils. *Geophysical Research Letters*, 31, L09501, doi:10.1029/2004GL019485.

Retta, A., L. E. Wagner, J. Tatarko, and T. C. Todd. 2013. Evaluation of bulk density and vegetation as affected by military vehicle traffic at Fort Riley, Kansas. *Transactions of the ASABE*, 56(2): 653-665.

Rice, M. A., B. B. Willetts, and I. K. McEwan. 1996. Wind erosion of crusted soil sediments. *Earth Surface Processes and Landforms*, 21(3): 279-293.

SAS Institute Inc. 2011.Online Documentation. Retrieved from: (http://support.sas.com/documentation/onlinedoc/stat/)

Schlichting, H., and K. Gersten. 2000. Boundary Layer Theory, 8th, Springerrlag, Berlin, Germany.

Schwartz, J., D. W. Dockery, and L. M. Neas. 1996. Is daily mortality associated specifically with fine particles? *Journal of the Air and Waste Management Association*, 46(10): 927-939.

Shao Y, M.R. Raupach, and P.A. Findlater. 1993. Effect of saltation bombardment on the entrainment of dust by wind. *Journal of Geophysical Research* 98(D7): 12719 – 12726.

Sharratt, B. S., and D. Lauer. 2006. Particulate matter concentration and air quality affected by windblown dust in the Columbia Plateau. *Journal of environmental quality*, 35(6): 2011-2016.

Sloneker, L.L, and W.C. Moldenhauer. 1977. Measuring the amount of crop residue remaining after tillage. *Journal of Soil Water Conservation*, 32: 231-236.

Stetler, L. D. 1997. An isokinetic sampler for wind tunnel use. ASAE Meeting Paper No. 97-2031. American Society of Agricultural Engineers, St. Joseph, MI.

Sweeney, M., V. Etyemezian, T. Macpherson, W. Nickling, J. Gillies, G. Nikolich, and E. McDonald. 2008. Comparison of PI-SWERL with dust emission measurements from a straight-line field wind tunnel. *Journal of Geophysical Research*, 113(F1): 1–12. doi:10.1029/2007JF000830.

Sweeney, M. R., E. V. McDonald, and V. Etyemezian. 2011. Quantifying dust emissions from desert landforms, eastern Mojave Desert, USA.*Geomorphology*, 135(1): 21-34.

Timonen, K. L., E. Vanninen, J. De Hartog, A. Ibald-Mulli, B. Brunekreef, D. R. Gold, and J. Pekkanen. 2006. Effects of ultrafine and fine particulate and gaseous air pollution on cardiac autonomic control in subjects with coronary artery disease: the ULTRA study. *Journal of Exposure Science and Environmental Epidemiology*, 16(4): 332-341.

US-DoD. 2013. Base structure report: FY 2013 Baseline. Available at: http://www.acq.osd.mil/ie/download/bsr/Base%20Structure%20Report%202013_Baseline%2030%20Sept%202012%20submission.pdf . Accessed: 20 Nov., 2013.

US-EPA. 2011. *National Ambient Air Quality Standards (NAAQS).* Retrieved from: http://www.epa.gov/air/criteria.html.

Wagner L. E. and Y. Yu. 1991. Digitization of profile meter photographs. *Transactions of the ASAE,* 34(2): 412–416.

Woodruff, N.P. and F.H. Siddoway.1965. A wind erosion equation. Soil Science Society Am. Proc. 29, 602 – 608.

Yamaguchi, N., A. Sakotani, T. Ichijo, T. Kenzaka, K. Tani, T. Baba, and M. Nasu. 2012. Break down of asian dust particle on wet surface and their possibilities of cause of respiratory health effects. *Biological and Pharmaceutical Bulletin,* 35(7): 1187-1190.

Zobeck, T. M. 1991a. Soil properties affecting wind erosion. *Journal of Soil and Water Conservation, 46*: 112-118.

Zobeck, T. M. 1991b. Abrasion of crusted soils: Influence of abrader flux and soil properties. *Soil Science Society of America Journal*, 55(4): 1091-1097.

Zobeck, T. M., and D. W. Fryrear. 1986. Chemical and physical characteristics of windblown sediment. II. Chemical characteristics and total soil and nutrient discharge. *Transactions of the ASAE,* 29: 1037-1044.

Zobeck, T. M., and C. A. Onstad. 1987. Tillage and rainfall effects on random roughness: a review. *Soil and Tillage Research,* 9(1): 1-20.